The Stepwise Reaction of Rhodium and Iridium Complexes of formula [$MCl_2(\kappa^4$*C,N,N',P*−L)] with Silver Cations: A Case of *trans*-Influence and Chiral Self-Recognition

María Carmona,[a] Leyre Tejedor,[a] Ricardo Rodríguez,*[a] Vincenzo Passarelli,*[a,b] Fernando J. Lahoz,[a] Pilar García-Orduña[a] and Daniel Carmona*[a]

Abstract: Acetonitrile suspensions of the dichlorido complexes [$MCl_2(\kappa^4$*C,N,N',P*−**L**)] (M = Rh (**1**), Ir (**2**)) react with $AgSbF_6$ in a 1/2 molar ratio affording the bis-acetonitrile complexes [$M(\kappa^4$*C,N,N',P*−**L**)$(NCMe)_2][SbF_6]_2$ (**3**, **4**). The reaction takes place in a sequential manner. In a 2/1 molar ratio, it affords the dimetallic monochlorido-bridged compounds [{$MCl(\kappa^4$*C,N,N',P*−**L**)$\}_2(\mu$-Cl)][SbF_6] (**5**, **6**). In a 1/1 molar ratio, the monosubstituted solvato-complexes [$MCl(\kappa^4$*C,N,N',P*−**L**)(Solv)][SbF_6] (Solv = H_2O, MeCN, **7**-**10**) were obtained. Finally, in a 2/3 molar ratio, it gives complexes **11** and **12** of formula [{$M(\kappa^4$*C,N,N',P*−**L**)(NCMe)$(\mu$-Cl)$\}_2$Ag][$SbF_6]_3$ in which a silver cation joints two cationic monosubstituted acetonitrile-complexes [$MCl(\kappa^4$*C,N,N',P*−**L**) (NCMe)]$^+$ through the remaining chlorido ligands and two Ag···C interactions with one of the phenyl rings of each PPh_2 group. In all the complexes, the aminic nitrogen and the central metal atom are stereogenic centers. In the trimetallic complexes **11** and **12**, the silver atom is also a stereogenic center. The configuration at the silver is predetermined by the configuration of the rhodium or iridium fragments. The

[a] M. Carmona, L. Tejedor, Dr. R. Rodríguez, Dr. V. Passarelli, Prof. Dr. F. J. Lahoz, Dr. P. García-Orduña, Prof. Dr. Daniel Carmona
Departamento de Catálisis y Procesos Catalíticos
Instituto de Síntesis Química y Catálisis Homogénea (ISQCH), CSIC - Universidad de Zaragoza
Departamento de Química Inorgánica
Pedro Cerbuna 12, 50009 Zaragoza, Spain
E-mail: dcarmona@unizar.es

[b] Dr. V. Passarelli
Centro Universitario de la Defensa
Ctra. Huesca s/n, 50090 Zaragoza, Spain

Supporting Information for this article can be found under http://.....

arrangement of the four coordinating atoms of the tetradentate ligand **L** is retained throughout the chlorido abstraction process. This is compatible with the retention of the absolute configuration of the complexes. The formation of the cation of the dimetallic complexes **5** and **6**, as well as that of the trimetallic complexes **11** and **12**, takes place with chiral molecular self-recognition: only di or trimetallic complexes containing monometallic fragments with the same absolute configuration at the metal and at the nitrogen atoms within each moiety have been detected R-X polvo. Experimental data and DFT calculations provide plausible explanations for the observed molecular recognition. The new complexes have been characterized by analytical and spectroscopic means and by X-ray diffraction methods for the compounds **3**, **5**, **10**, **11** and **12**.

Introduction

Metal complexes are extensively used as one of the most powerful approaches for the catalytic synthesis of nonracemic chiral compounds. Typically, a chiral environment is generated around the metal by coordination of enantiopure organic ligands and centered, axial or planar chirality, residing in the ligands, is transferred to the substrates.[1] Taking into account that the most common manner in which substrates are activated toward chemical transformations is through metal coordination, it seems reasonable to assume that catalysts based on stereogenic metal centers would offer the most promising approach for achieving efficient transfer of chirality during an asymmetric process.[2]

Reactions mediated by Lewis acid metal complexes necessarily involve the formation and cleavage of chemical bonds in which the metal is implicated, with the concomitant potential erosion of the metal enantiopurity. Moreover, a major requirement for metallic catalyst precursors is the existence of coordination position(s) available for the substrates, these positions being usually occupied by solvent molecules. In summary, a good candidate for catalyst containing a metal center as source of chirality has to be substitutionally labile but stereochemically stable. Building up metallic complexes fulfilling both requirements at once is a challenging task.

To tackle this problem, we contemplate the possibility of preparing octahedral complexes of the d^6 metal ions Rh^{+3} and Ir^{+3} bearing tetradentate ligands. The resulting tetracoordinate frame would be responsible of maintaining the configuration at the metal whereas the two remaining coordination sites would be available for catalytic transformations.

Catalysts based on metal complexes containing tetradentate ligands have been extensively studied. Paradigmatic examples of ligands employed to this end are salen and

related derivatives with an ONNO set of donor atoms,[3] bisphosphane-bisimine or bisamine compounds containing a PNNP donor set[4] and a variety of nitrogenated compounds bearing a N_4 donor set.[5]

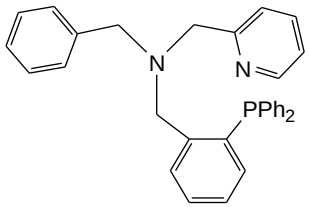

Scheme 1. Tripodal tetradentate tertiary amine **HL**.

In this context, we selected the tetradentate tripodal ligand **HL** (Scheme 1) in which a tertiary amine bears three different substituents i. e. a pyridine ring, a diphenylphosphane group and an aromatic ring with *ortho* positions available for metalation. This ligand is able to coordinate to an octahedral metal keeping the two remaining coordination sites mutually *cis* as it has been shown in the dichlorido compounds [MCl_2(κ^4*C,N,N',P*–**L**)] (M = Rh (**1**), Ir (**2**)) that we have recently prepared[6] as racemic mixtures of the (*R*$_{Nam}$)-*OC*-6-54-*C* and (*S*$_{Nam}$)-*OC*-6-54-*A*[7,8] isomers (Scheme 2).

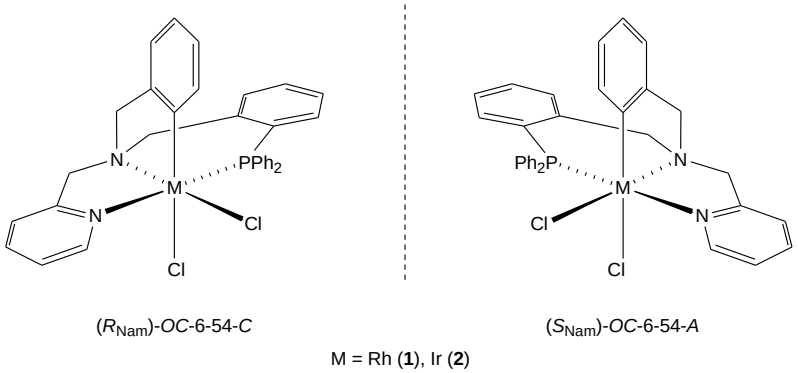

Scheme 2. (*R*$_{Nam}$)-*OC*-6-54-*C* and (*S*$_{Nam}$)-*OC*-6-54-*A* enantiomers of the dichlorido rhodium and iridium compounds [MCl_2(κ^4*C,N,N',P*–**L**)].

The ligand topology makes interdependent the configuration at the metal and at the aminic nitrogen center and only up to three pair of enantiomers can form. DFT calculations[6] showed that the isomer in which the phosphorus atom is *trans* to the

pyridinic nitrogen is the most stable and, notably, only this pair of enantiomers (Scheme 2) was detected and isolated.[6]

As for octahedral bis-cyclometalated rhodium(III) and iridium(III) complexes, a high thermal and configurational stability is expected for their congeners bearing tripodal tetradentate ligands.[9] Hence, a retention of the configuration in the course of subsequent transformations can be envisaged, which is undoubtedly an important feature from the point of view of an efficient transmission of chirality.

As stated above, to get suitable catalyst precursors, the chlorido ligands of these complexes have to be replaced by labile ligands such as solvent molecules. Silver salt metathesis is the widely preferred method of halide abstraction to generate transition-metal fragments with vacant sites.[10] However, despite the widespread use of this method, it is not free of shortcomings. Incomplete chloride abstraction, leading to dinuclear bridged chlorido complexes, or formation of silver containing heteronuclear complexes are among the most common disadvantages.[10]

We here wish to report the results obtained in the reaction of the dichlorido complexes [$MCl_2(\kappa^4$*C,N,N',P*–**L**)] with silver hexafluoroantimoniate on route to labile solvato-complexes of formula [$M(\kappa^4$*C,N,N',P*–**L**)$(Solv)_2]^{2+}$. A detailed study of the course of the reaction reveals that it takes place in a sequential manner. In fact, we show here that mono- di- and trinuclear intermediates are involved in the process. Interestingly, the complete characterization of these intermediates unveils that the formation of the polynuclear species is completely diastereoselective with chiral self-recognition between the involved chiral fragments R-X polvo. Moreover, in the silver containing trinuclear intermediates, the silver cation presents an unusual distorted-tetrahedral chiral

environment with predetermined chirality.[5d,e] DFT calculations, also included in this article, support the observed stereoselectivity.

Results and Discussion

Reaction of [$MCl_2(\kappa^4 C,N,N',P-L)$] (M = Rh (1), Ir (2)) with $AgSbF_6$ in 1/2 molar ratio

Refluxing acetonitrile suspensions of the racemic rhodium complex **1** in the presence of $AgSbF_6$ (molar ratio 1/2) for 40 h afforded the cationic bis-acetonitrile complex $[Rh(\kappa^4 C,N,N',P-\mathbf{L})(NCMe)_2][SbF_6]_2$ (**3**) in 92 % isolated yield. The iridium homologue $[Ir(\kappa^4 C,N,N',P-\mathbf{L})(NCMe)_2][SbF_6]_2$ (**4**) was isolated, in 79 % yield, by treating a suspension of the racemic dichlorido $[IrCl_2(\kappa^4 C,N,N',P-\mathbf{L})]$ (**2**), in acetonitrile, with two moles of $AgSbF_6$, at 130 ºC in a sealed tube, for 4 days (Eq. 1).

$$[MCl_2(\kappa^4 C,N,N',P\text{-}\mathbf{L})] \;(M = Rh\ (\mathbf{1}),\ Ir\ (\mathbf{2})) \;+\; 2\ AgSbF_6 \xrightarrow[-\ 2\ AgCl]{MeCN,\ \Delta} [M(\kappa^4 C,N,N',P\text{-}\mathbf{L})(NCMe)_2][SbF_6]_2 \;(M = Rh\ (\mathbf{3}),\ Ir\ (\mathbf{4})) \qquad (1)$$

The compounds were characterized by analytical and spectroscopic methods (see Experimental Section) and by the X-ray determination of the crystal structure of the rhodium compound **3** (vide infra). The metal atom and the aminic nitrogen of the ligand are stereogenic centers. However, the NMR spectra of complexes **3** and **4** consist of only one set of sharp resonance signals. Taking into account that the samples of the starting compounds **1** and **2** were racemic mixtures of R_N,C_M and S_N,A_M isomers[8] (Scheme 2), compounds **3** and **4** should have been obtained as racemic mixtures of only

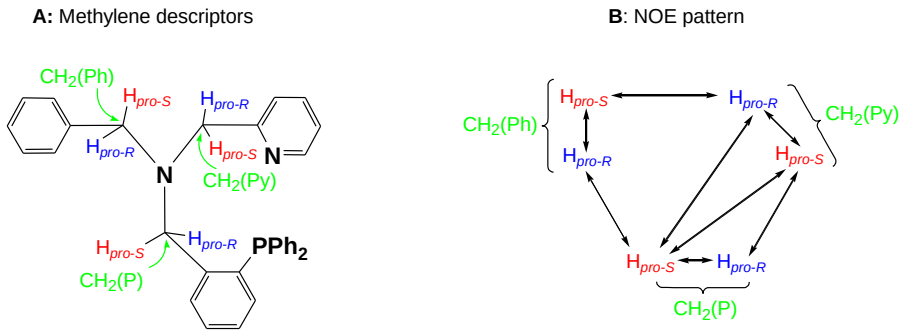

Scheme 3. Assignment of the methylene descriptors (**A**) and NOE pattern (**B**) on (R_{Nam})-*OC*-6-35-*C* isomers of complexes **3** and **4**.

one of the three possible isomers. The geometry of the isolated isomer can be unveiled by NMR measurements. The value of the *J*(PH) coupling constants together with COSY, HSQC and HMBC experiments permit the assignment of the six diastereotopic protons which have been labeled as CH_2(Py), CH_2(Ph) and CH_2(P) (see Scheme 3**A**). Scheme 3**B** shows the NOE pattern measured for these six methylene protons. Additionally, the methyl protons of the acetonitrile ligand *trans* to the aminic nitrogen atom exhibit NOE relationship with the 6-CH(Py) and 6-CH(Ph) protons of the tetradentate ligand (see Scheme 4). All these NMR data are only compatible with the pair of enantiomers (R_{Nam})-*OC*-6-35-*C* (R_N,C_M) and (S_{Nam})-*OC*-6-35-*A* (S_N,A_M) in which the phosphorus and the pyridine nitrogen atoms are mutually *trans* (Scheme 4). Accordingly, a *J*(PH) coupling constant of about 4.6 Hz (complex **3**) or 5.7 Hz (complex **4**) was measured for the proton-6 of the pyridine moiety (6-CH(Py)). Hence, we propose that compounds **3** and **4** have been obtained as racemic mixtures of the isomers R_N,C_M and S_N,A_M shown in Scheme 4 as, in fact, it has been corroborated by the X-ray determination of the crystal structure of compound **3**.

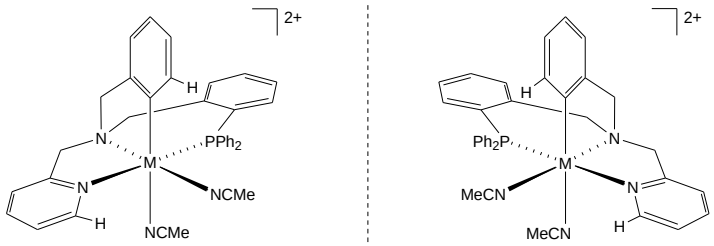

(R_{Nam})-*OC*-6-35-*C*
M = Rh (**3**), Ir (**4**)

(S_{Nam})-*OC*-6-35-*A*
M = Rh (**3'**), Ir (**4'**)

Scheme 4. Isolated enantiomers of the complexes **3** and **4**.

Single crystals of **3**, suitable for X-ray analysis, were obtained from dichloromethane solutions of the compound. A view of the structure of the cation of the complex is depicted in Figure 1 and relevant characteristics of the metal coordination sphere are summarized in Table 1.

The cation exhibits a distorted-octahedral coordination geometry around the central metal atom. Two acetonitrile ligands coordinated through the nitrogen atom occupy two *cis* coordination sites and four ligating atoms of the tetradentate ligand complete the coordination metal sphere. As indicated by solution NMR data, the phosphorus atom is *trans* to the pyridinic nitrogen N(2), while the nitrile nitrogen atoms N(3) and N(4) are found to be *trans* to the aminic nitrogen N(1) and to the aromatic C(28) carbon atoms, respectively.

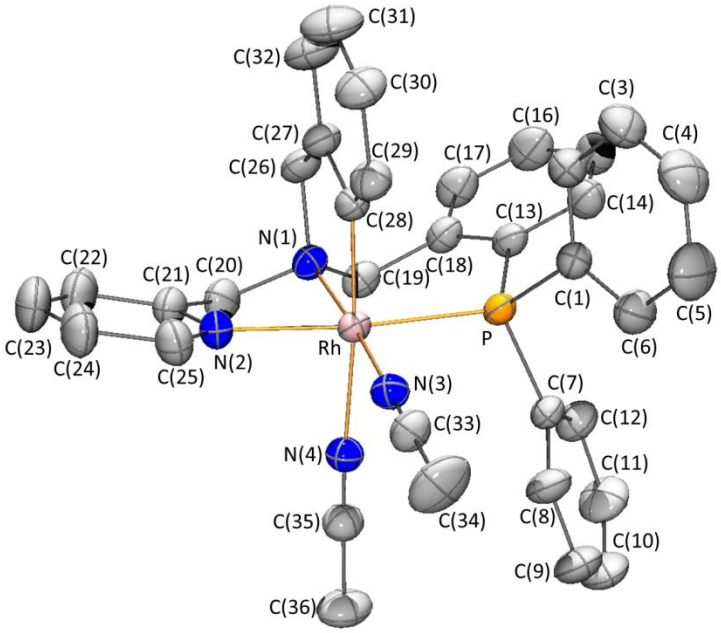

Figure 1. Molecular structure of the cation of complex **3** (thermal ellipsoids at a 30% probability level). Only the (R_{Nam})-*OC*-6-35-*C* enantiomer is shown. For clarity, hydrogen atoms have been omitted.

Table 1. Bond lengths (Å) and angles (°) for complex **3/3'.**

Rh-P	2.2941(12)	N(1)-Rh-N(2)	81.34(16)
Rh-N(1)	2.069(4)	N(1)-Rh-N(3)	175.08(16)
Rh-N(2)	2.099(4)	N(1)-Rh-N(4)	92.96(16)
Rh-N(3)	2.022(4)	N(1)-Rh-C(28)	84.46(18)
Rh-N(4)	2.187(4)	N(2)-Rh-N(3)	93.92(16)
Rh-C(28)	2.005(4)	N(2)-Rh-N(4)	90.21(16)
P-Rh-N(1)	93.86(11)	N(2)-Rh-C(28)	85.30(17)
P-Rh-N(2)	174.08(12)	N(3)-Rh-N(4)	88.36(16)
P-Rh-N(3)	90.79(11)	N(3)-Rh-C(28)	93.87(18)
P-Rh-N(4)	93.52(12)	N(4)-Rh-C(28)	175.11(17)
P-Rh-C(28)	90.81(13)		

The complex crystallizes in the *C2/c* centrosymmetric space group and, therefore, pairs of enantiomers, specifically the R_N,C_M (**3**) and S_N,A_M (**3'**) isomers[8] (see Scheme 3) are present in its unit cell.

Structural features of complex **3** are very close to those of the parent dichlorido compound **1**.[6] As a consequence of the strong *trans* influence of the sp^2 carbon atom, the Rh−N(4) bond length is 0.165(6) Å longer than that of the Rh−N(3) bond. The tetradentate coordination of the ligand **L** leads to the formation of two five-membered and one six-membered metalacycles.[11] In the R_N,C_M enantiomer **3**, the Rh-N(1)-C(20)-C(21)-N(2) metalacycle exhibits an E_2 envelope conformation slightly distorted toward a $^3T_2$ conformation, the Rh-N(1)-C(26)-C(27)-C(28) metalacycle is almost planar, as indicated by the value of the puckering amplitude (0.032(5) Å), and the six-membered metalacycle shows a screw-boat disposition ($^5S_6$) with a slight distortion towards a $^2T_6$ conformation.[12]

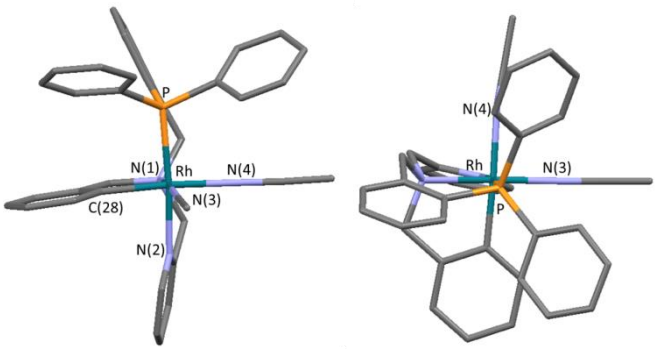

Figure 2. Views of the isomer of configuration (R_{Nam})-*OC*-6-35-*C* of the complex **3** along the Rh−N(1) and P−Rh directions.

Taking into account the potential application of these compounds as catalyst precursors in asymmetric transformations, it is interesting to point out that the phenyl groups of the phosphano arm of the ligand **L** shields one of the faces of the plane defined by the metal atom and the two acetonitrile ligands. However, the other face of this plane remains essentially clear (Figure 2). Hence, if a prochiral substrate replaces one or two

acetonitrile ligands, one of its enantiofaces would be more shielded than the other and, therefore, enantioselective attacks would be anticipated.

Sequential reactivity of the dichlorido complexes 1 and 2 with silver cations

NMR spectra show the formation of several metallic intermediates over the course of the reaction leading to the solvato complexes **3** and **4**. When dealing with the mechanism of formation of these complexes, it is worth mentioning that in the starting compound the chlorido ligands are located one *trans* to the aminic nitrogen and the other *trans* to a metalated carbon atom of a phenyl ring. The strong difference in *trans* influence between these two organic functions gives rise to M−Cl bond lengths more than 0.1 Å longer for the M−Cl bond *trans* to the carbon atom than for the M−Cl bond *trans* to the nitrogen atom.[6] Consequently, it may be envisaged that the abstraction of the former chlorido ligand would be preferential over the abstraction of the latter (vide infra).

$$2\ [MCl_2(\kappa^4\textit{C,N,N',P}\text{-}\mathbf{L})] \quad (M = Rh\ (\mathbf{1}),\ Ir\ (\mathbf{2})) \quad + \quad AgSbF_6 \xrightarrow[-\ AgCl]{CH_2Cl_2,\ RT} [\{MCl(\kappa^4\textit{C,N,N',P}\text{-}\mathbf{L})\}_2(\mu\text{-}Cl)][SbF_6] \quad (M = Rh\ (\mathbf{5}),\ Ir\ (\mathbf{6})) \qquad (2)$$

Trying to clarify this point, $AgSbF_6$ was added to dichloromethane solutions of **1** and **2**, in a 2/1 molar ratio, at room temperature. After 2 h under these conditions, solids of formula $[\{MCl(\kappa^4\textit{C,N,N',P}\text{−}\mathbf{L})\}_2(\mu\text{-Cl})][SbF_6]$ (M = Rh (**5**), Ir (**6**)) were isolated from the reaction medium in good yield (Eq. 2).

Single crystals suitable for X-ray analysis were obtained from dichloromethane solutions of the rhodium compound **5**. The X-ray structure reveals that the complex cation contains two $Rh(\kappa^4\textit{C,N,N',P}\text{−}\mathbf{L})Cl$ moieties bridged by a chlorido ligand (Figure 3). The Rh(1)···Rh(2) distance (4.7833(6) Å) excludes any significant metal-metal interaction. The metal atoms and the aminic nitrogens are stereogenic centers. As the

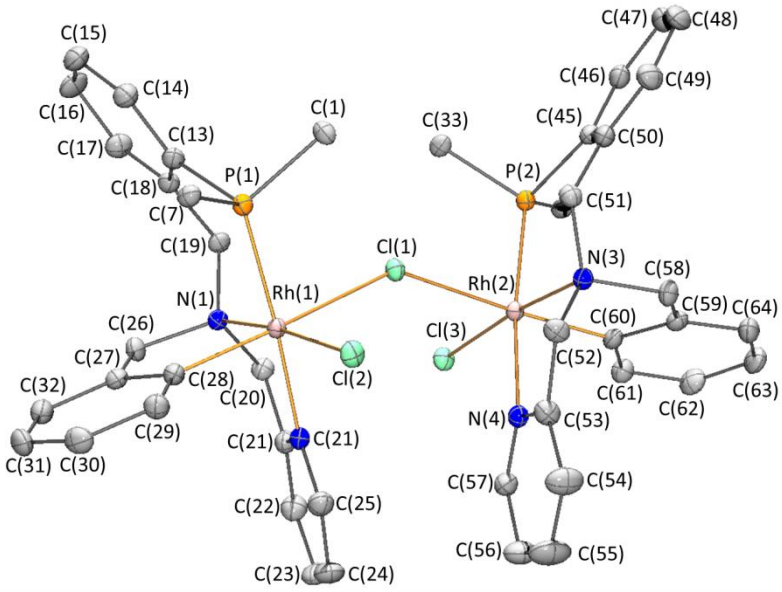

Figure 3. Molecular structure of the cation of complex **5**. Only the cation with (R_{Nam})-*OC*-6-65-*C* configuration in both metallic moieties is shown. For clarity hydrogen atoms have been omitted and only the *ipso* carbons of the PPh_2 groups are shown.

Table 2. Bond lengths (Å) and angles (°) for complex **5/5'**

Rh(1)-Cl(1)	2.5516(6)	Rh(2)-Cl(1)	2.5343(6)
Rh(1)-Cl(2)	2.3625(6)	Rh(2)-Cl(3)	2.3517(6)
Rh(1)-P(1)	2.2757(7)	Rh(2)-P(2)	2.2681(7)
Rh(1)-N(1)	2.085(2)	Rh(2)-N(3)	2.086(2)
Rh(1)-N(2)	2.093(2)	Rh(2)-N(4)	2.092(2)
Rh(1)-C(28)	2.001(2)	Rh(2)-C(60)	1.999(2)
Cl(1)-Rh(1)-Cl(2)	91.15(2)	Cl(1)-Rh(2)-Cl(3)	91.57(2)
Cl(1)-Rh(1)-P(1)	89.19(2)	Cl(1)-Rh(2)-P(2)	92.89(2)
Cl(1)-Rh(1)-N(1)	89.02(6)	Cl(1)-Rh(2)-N(3)	89.60(6)
Cl(1)-Rh(1)-N(2)	92.59(6)	Cl(1)-Rh(2)-N(4)	91.72(6)
Cl(1)-Rh(1)-C(28)	172.79(7)	Cl(1)-Rh(2)-C(60)	173.68(7)
Cl(2)-Rh(1)-P(1)	91.34(2)	Cl(3)-Rh(2)-P(2)	91.46(2)
Cl(2)-Rh(1)-N(1)	173.01(6)	Cl(3)-Rh(2)-N(3)	173.77(6)
Cl(2)-Rh(1)-N(2)	92.41(6)	Cl(3)-Rh(2)-N(4)	92.89(6)
Cl(2)-Rh(1)-C(28)	95.98(7)	Cl(3)-Rh(2)-C(60)	94.74(7)
P(1)-Rh(1)-N(1)	95.65(6)	P(2)-Rh(2)-N(3)	94.59(6)
P(1)-Rh(1)-N(2)	175.81(6)	P(2)-Rh(2)-N(4)	173.57(6)
P(1)-Rh(1)-C(28)	91.72(7)	P(2)-Rh(2)-C(60)	87.33(7)
N(1)-Rh(1)-N(2)	80.60(8)	N(3)-Rh(2)-N(4)	80. 96(8)
N(1)-Rh(1)-C(28)	83.77(9)	N(3)-Rh(2)-C(60)	84.10(9)
N(2)-Rh(1)-C(28)	86.04(9)	N(4)-Rh(2)-C(60)	87.60(9)

compound was found to crystallize in the centrosymmetric $P2_1/n$ space group, an equimolar mixture of the enantiomers, **5** and **5'** is present in its unit cell. Notably, within each cation both metallic moieties adopt the same absolute configuration i. e. both present

(R_{Nam})-*OC*-6-65-*C* (**5**) or (S_{Nam})-*OC*-6-65-*A* (**5'**) configuration. Only the unprimed isomer **5** is shown in Figure 3. Some structural parameters of the metal coordination are listed in Table 2. They nicely agree with those reported for the parent dichlorido complex **1**.[6] A non-crystallographic binary axis, passing through the bridging chlorine atom, relates the two moieties of the dinuclear molecule.

Formally, the dinuclear cation is the result of the dissociation of the chlorido ligand *trans* to the sp^2 coordinated carbon atom in the starting complex [$RhCl_2(\kappa^4 C,N,N',P$–**L**)] followed by the coordination at the generated vacant site of the chlorido ligand *trans* to the sp^2 coordinated carbon atom of a second molecule of **1**. The linkage isomer in which the bridging chlorido is *trans* to one aminic nitrogen and one carbon atom was not detected. The terminal rhodium chlorido (*trans* to an aminic nitrogen) bond lengths (Rh(1)−Cl(2) 2.3625(6) Å, Rh(2)−Cl(3) 2.3517(6) Å) are significantly shorter than those of the rhodium bridging chlorido (*trans* to an sp^2 carbon atom, (Rh(1)−Cl(1) 2.5516(6) Å, Rh(2)−Cl(1) 2.5343(6) Å). The elongation of the latter bond lengths should be reasonably due to the *trans* influence together with the fact that in complex **5** both metal atoms are sharing the bridging chloride charge density. In fact, they are longer than the terminal Rh−Cl bond, *trans* to sp^2 carbon atoms, of the parent dichlorido mononuclear compound **1** (2.5222(12) Å).

Unsupported chloride bridges are not very frequent in dinuclear Rh/Ir complexes and their structural parameters have been mainly related to steric constraints of the metal environment.[13] The Rh(1)−Cl(1)−Rh(2) angle in **5** (140.28(3)º) is similar to those reported for related octahedral Rh/Ir complexes bearing bulky ligands with an unsupported chloride bridge: [{RhClMe(^{i}Pr-pybox)}$_2$(μ-Cl)]$^+$ (138.15(7)º),[14] [{IrH[{PPh_2(*o*-C_6H_4CO)}$_2$H]}$_2$(μ-Cl)]$^+$ (130.3(1)º),[15] [{IrCl(C_2H_5)(^{i}Pr-pybox)}$_2$(μ-

Cl)]$^+$ (139.17(11)º),[16] [{$IrH_2(PMe_3)_3$}$_2$(μ-Cl)]$^+$ (139.6(3)º).[13b] In complex **5**, the value of the Rh−Cl−Rh angle allows the separation of the two bulkiest PPh_2 fragments as well as the approach of the two pyridine rings via non-covalent π···π intramolecular interactions. Indeed, the centroid-centroid distance between the pyridine rings is 4.0041(16) Å and the dihedral angle between their mean planes is of only 14.68(13)°. This arrangement is similar to that found in related metallic complexes containing π···π stacked heterocycles.[17] Furthermore, the ring planes are offset in such a way that the C(25) and C(57) carbon atoms lie near over the center of the other pyridine ring and their hydrogen atom is placed almost on the top of a pyridine ring C=C bond (Figure 4). This slipped π···π stacking is characterized by offset angles of 23.7 and 31.0° between the ring normals and the vector between the centroids.

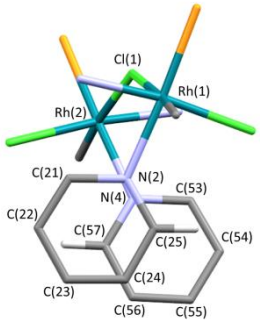

Figure 4. A view of the π···π stacking of the pyridine rings in complex **5**.

On the other hand, DOSY ^{1}H NMR measurements[18] were carried out in CD_2Cl_2 to obtain information about the nuclearity in solution of compounds **5** and **6**. For comparative purposes, the rhodium mononuclear compounds [$RhCl_2$(κ^4*C,N,N',P*–**L**)] (**1**)[6] and [RhCl(κ^4*C,N,N',P*–**L**)(NCMe)][SbF_6] (**9**) and their iridium homologues **2** and **10**, respectively, were also studied. The preparation and characterization of complexes **9** and **10** is reported below. The translational self-diffusion coefficients (D_t, Table 3) show that **5** and **6** diffuse slower than **1**, **2**, **9** and **10** and that the diffusion coefficients ratio between the latter and the former (in the range 1.24-1.35) is very close to the ideal

calculated value (1.26) for diffusing species with a 2-fold volume one respect to the other. Accordingly, the hydrodynamic radii of complexes **1**, **2**, **9**, and **10** (r_H, Table 3) exhibit values in the 4.71-5.07 Å range. However, r_H values of 6.27 and 6.36 Å were determined for complexes **5** and **6**, respectively. In summary, the performed diffusion experiments support a dinuclear structure for complexes **5** and **6** in dichloromethane solution.

Table 3. Diffusion coefficient (D_t, m^2s^{-1}), hydrodynamic radius (r_H, Å) for compounds **1**, **2**, **9**, **10**, **5** and **6**.

Comp.	10^{10} D_t	r_H
1	10.78	4.71
2	10.06	5.05
9	10.60	4.79
10	10.01	5.07
5	8.100	6.27
6	7.986	6.36

Conditions: CD_2Cl_2, 293 K, 7.75 × 10^{-3} mM. Solvent viscosity: 0.43 cP at 293 K.

However, the NMR spectra of **5** and **6**, in the presence of substoichiometric amounts of donor solvents, such as water or acetonitrile, indicate that the complexes asymmetrically split into the neutral dichlorido compounds [MCl_2(κ^4*C,N,N',P*–**L**)] (**1**, **2**) and the cationic solvato-complexes [MCl(κ^4*C,N,N',P*–**L**)(Solv)]$^+$ (Solv = H_2O; M = Rh (**7**), Ir (**8**). Solv = NCMe; M = Rh, (**9**), Ir (**10**) Scheme 5) and that the metallic fragments are in equilibrium in dichloromethane solution. The solvato-complexes **7**-**10** have been independently prepared following an alternative route (vide infra). As a confirmation, the equilibrium of Scheme 5 was also achieved by mixing equimolar amounts of isolated dichlorido compounds **1** or **2** with the corresponding cationic compounds **7**/**8** or **9**/**10**.

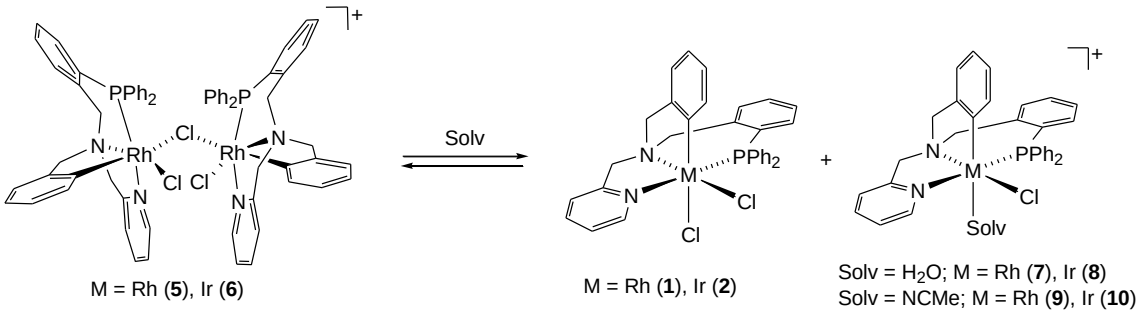

Scheme 5. Solution equilibrium for complexes **5** and **6**.

Notably, ^{1}H-^{1}H EXSY cross-peaks reveal the exchange between corresponding nuclei of the dichlorido and solvato-complexes and those of the dimetallic complexes **5** and **6** (see SI). It is noteworthy to point out that the sole isomer observed for compounds **5** and **6** is the same as the one obtained from complexes **1** and **2** according to Eq. 2. The X-ray molecular structure of complex **5** reveals that the configuration of each metallic moiety within the dinuclear cation is the same: R_N,C_M or S_N,A_M (see above). Hence, the reaction between the dichlorido compounds and the aquo or acetonitrile solvato-complexes to afford the dinuclear compounds **5** and **6** (see Scheme 5) takes place with molecular self-recognition: only dimetallic cations of absolute configuration R_N,C_M,$R_{N'}$,$C_{M'}$ or S_N,A_M,$S_{N'}$,$A_{M'}$ form.[19]

The solid state molecular structure of complex **5** reveals that π···π interactions between the two pyridine rings of the molecule are operating (see above). Most probably, these interactions are maintained in solution because, in complexes **5** and **6**, the resonance peak attributed to the 6-CH(Py) proton appears 1.18 and 1.17 ppm upfield shifted with respect to that assigned to this proton in the starting mononuclear complexes **1** and **2**, respectively. This shift should be attributed to the shielding produced by the diamagnetic electronic current of the other pyridine group (see Figure 4).

DFT calculations on complexes 5 and 6

DFT calculations were carried out in order to assess the relative stability of the possible isomers of the cations **I**-**IV** of formula [{MCl(κ^4*C,N,N',P*–**L**)}$_2$(μ-Cl)]$^+$ (M = Rh, Ir). Figure 5 shows their calculated structures and relative free energies. As far as the metal environment is concerned, **III** and **IV** are linkage isomers of **I** and **II**, respectively. Indeed, both **I** and **II** contain two metalated carbon atoms *trans* to the bridging chlorido ligand, while the bridging chlorido ligand of **III** and **IV** is *trans* to the metalated carbon of one MCl(κ^4*C,N,N',P*–**L**) moiety and *trans* to the aminic nitrogen atom of the other

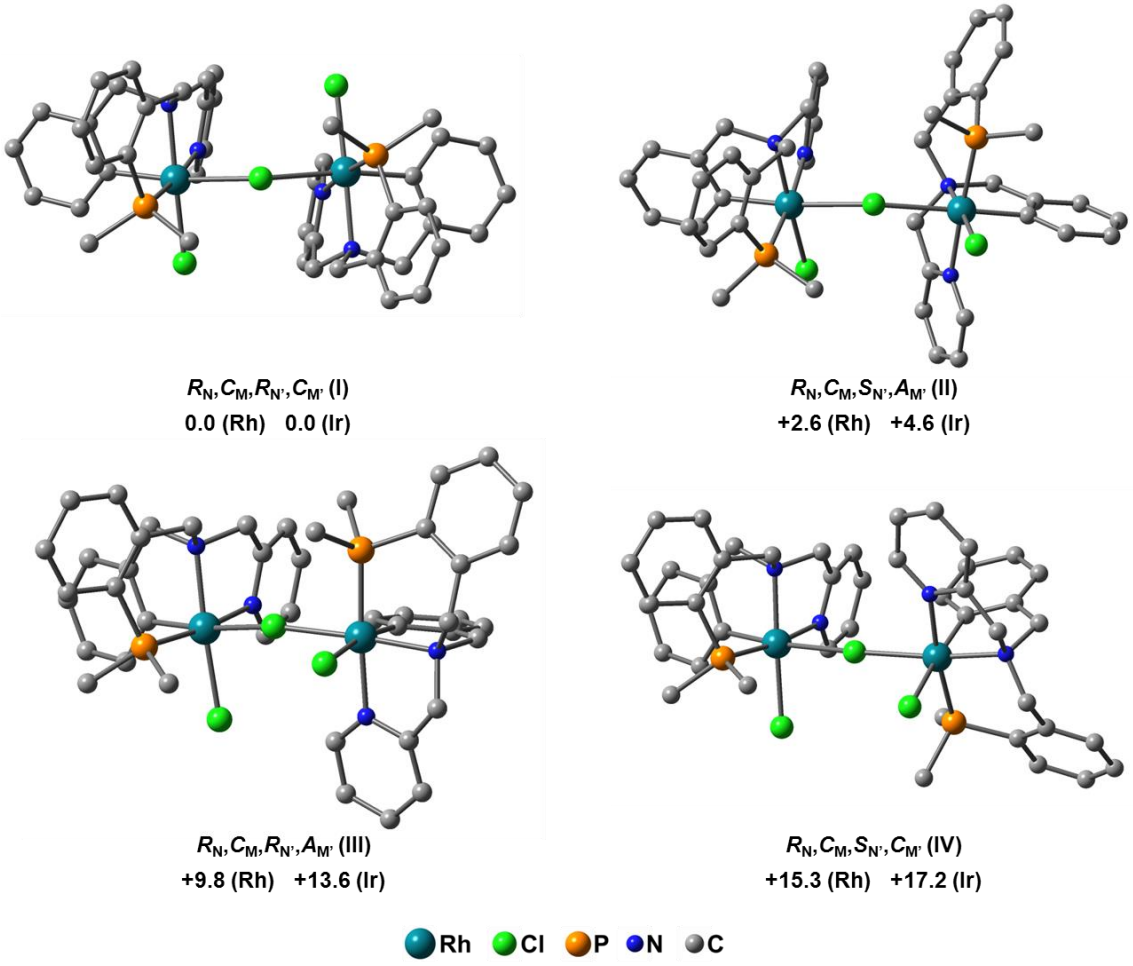

Figure 5. Structures and relative free energies (*G*, kcal·mol^{-1}, 298 K, CH_2Cl_2) of isomers **I**-**IV** of formula [{MCl(κ^4*C,N,N',P*-**L**)}$_2$(μ-Cl)]$^+$ (M = Rh, Ir). Only the structures with M = Rh are shown, those with M = Ir being similar. For clarity all hydrogen atoms are omitted and only *ipso* carbons of the PPh_2 moiety are shown.

moiety. When dealing with the configuration of the stereogenic centres, **I** and **III** contain two superimposable $MCl_2(CN_{am}N_{Py}P)$ moieties. On the other hand, **II** and **IV** contain two

$MCl_2(CN_{am}N_{Py}P)$ moieties with opposite configurations. Nevertheless, it should be noted that, as a consequence of the priority rules, the *C*/*A* descriptors assigned to isomers **III** and **IV** are different from those assigned to **I** and **II**.

For both rhodium and iridium, the isomers **III** and **IV** are observed at significantly higher free energies thus suggesting that its formation can be ruled out. Further, similar to the solid state structure of **5**, the most stable isomer **I** contains two equal configured (R_N,C_M)−$MCl_2(\kappa^4 C,N,N',P$–**L**) moieties and features a slipped π···π stacking of the pyridinic rings, similar to that above described for **5** (Figure 6).

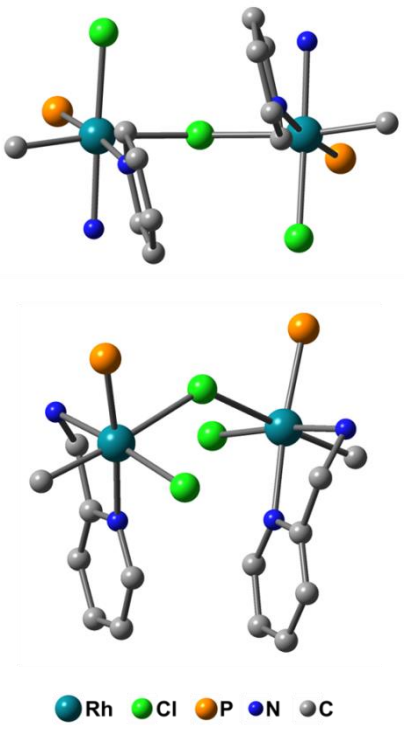

Figure 6. Views of the π···π stacking in **I**. Only the structure with M = Rh is shown, that with M = Ir being similar. Selected angles (º) and distances (Å) are: centroid-centroid distance 3.78 (Rh), 3.78 (Ir); dihedral angle between pyridinic rings 9.06 (Rh), 8.89 (Ir); averaged angle between ring normal and centroid-to-centroid vector 28.8 (Rh), 29.1 (Ir).

Accordingly, the isomer **II** with a configuration R_N,C_M,$S_{N'}$,$A_{M'}$ is less stable than **I** and, interestingly, features a mutual disposition of the MCl(κ^4*C,N,N',P*–**L**) moieties around the bridging chlorido ligand that prevents the stacking of the pyridinic moieties and, eventually, of any other pair of aromatic rings. Thus, for both metals, the stabilizing effect of the π···π stacking of the pyridinic moieties in **I** reasonably seems to be the key factor causing the higher stability of **I** with respect to **II**-**IV**. Consequently, this π···π stacking should be considered the origin of the molecular recognition leading to the regio- and stereoselective formation of **5** and **6** both in the reaction of **1** and **2** with $AgSbF_6$ in CH_2Cl_2 (Eq. 2) and in the reaction between **7**/**9** or **8**/**10** with **1** or **2** (Scheme 5).

Reaction of the dichlorido complexes 1 and 2 with $AgSbF_6$ in 1/1 molar ratio

Solutions of **1** and **2**, in wet dichloromethane, treated with $AgSbF_6$ in 1/1 molar ratio, at room temperature for two hours, afforded the cationic mononuclear aquo-complexes [MCl(κ^4*C,N,N',P*–**L**)(OH_2)][SbF_6] (M = Rh (**7**), Ir (**8**)). Under similar conditions, but employing acetonitrile as solvent, the acetonitrile complexes [MCl(κ^4*C,N,N',P*–**L**)(NCMe)][SbF_6] (M = Rh (**9**), Ir (**10**)) were isolated (Eq. 3a). Complexes **9** and **10** can also be prepared by adding $AgSbF_6$, in 1/1 molar ratio, to dichloromethane/acetonitrile solutions of the dinuclear compounds [{MCl(κ^4*C,N,N',P*–**L**)}$_2$(μ-Cl)][SbF_6] (M = Rh (**5**), Ir (**6**)) (Eq. 3b).

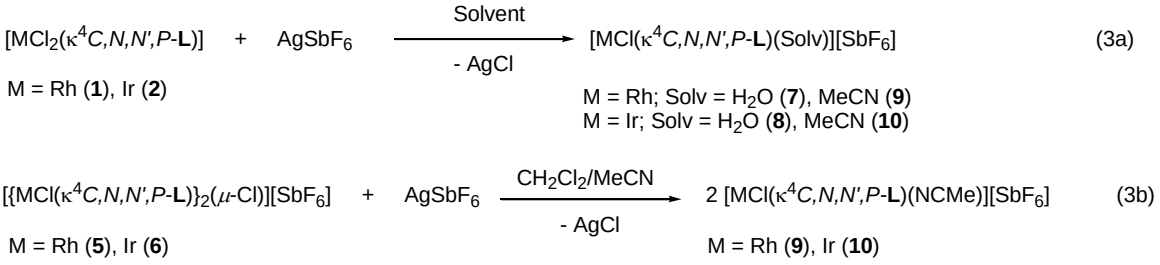

The NMR spectra of the mononuclear complexes **7**-**10** indicated that only one geometrical isomer has been isolated and NOESY experiments in solution and the X-ray determination of the crystal structure of the iridium complex **10** indicated that only the chlorido ligand *trans* to the phenyl carbon atom has been replaced with the solvent molecule.

Molecular structure of the compound [IrCl{(κ^4*C,N,N',P*–L)}(NCMe)][SbF$_6$] (10)

The crystal structure of complex **10** was determined by X-ray diffractometric methods. Single crystals were obtained from dichloromethane solutions of the complex. A view of the molecular structure is depicted in Figure 7 and relevant characteristics of the metal coordination sphere are summarized in Table 4.

As complexes **3** and **5**, compound **10** crystallizes in a centrosymmetric space group and therefore the crystal structure is found to be a racemate of enantiomers R_N,C_M (**10**) and S_N,A_M (**10'**). The asymmetric unit contains two crystallographically independent molecules. No statistically significant difference is observed in their bond lengths and angles.

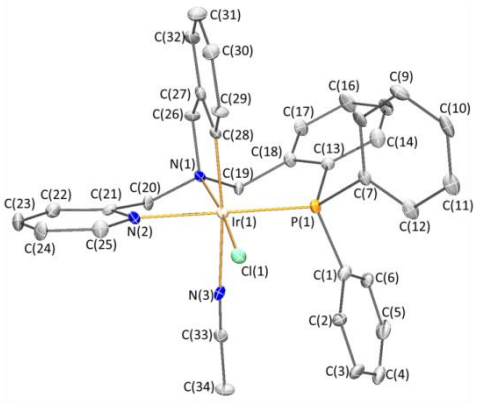

Figure 7. Molecular structure of the cation of complex **10**. Only the (R_{Nam})-*OC*-6-35-*C* enantiomer is shown. For clarity, hydrogen atoms have been omitted.

Table 4. Bond lengths (Å) and angles (°) for the two independent molecules of complex **10**/**10'**.

Ir(1)-Cl(1)	2.352(2)	2.360(2)	P(1)-Ir(1)-N(1)	95.83(19)	94.97(19)
Ir(1)-P(1)	2.267(2)	2.276(2)	P(1)-Ir(1)-N(2)	175.6(2)	175.8(2)
Ir(1)-N(1)	2.090(6)	2.102(7)	P(1)-Ir(1)-N(3)	91.65(19)	90.61(19)
Ir(1)-N(2)	2.098(7)	2.106(7)	P(1)-Ir(1)-C(28)	94.5(2)	96.6(2)
Ir(1)-N(3)	2.133(7)	2.104(7)	N(1)-Ir(1)-N(2)	80.1(3)	81.4(3)
Ir(1)-C(28)	2.011(8)	2.031(9)	N(1)-Ir(1)-N(3)	93.2(3)	93.3(3)
Cl(1)-Ir-P(1)	90.92(8)	91.08(7)	N(1)-Ir(1)-C(28)	83.3(3)	83.5(3)
Cl(1)-Ir(1)-N(1)	173.06(19)	173.73(19)	N(2)-Ir(1)-N(3)	87.0(3)	87.7(3)
Cl(1)-Ir(1)-N(2)	93.2(2)	92.7(2)	N(2)-Ir(1)-C(28)	86.7(3)	84.9(3)
Cl(1)-Ir(1)-N(3)	88.26(19)	88.31(19)	N(3)-Ir(1)-C(28)	173.2(3)	172.3(3)
Cl(1)-Ir(1)-C(28)	94.6(3)	94.2(3)			

The octahedral metal coordination environment reveals a $\kappa^4 C,N,N',P$ coordination of the ligand **L**, with structural features similar to those observed in the related complexes **3** and **5**. As a minor dissimilarity, the Ir-N-C-C-C metalacycle is slightly more deviated from the planarity in complex **10** than in complexes **3** and **5** (see SI). The coordinated acetonitrile is found to be *trans* to the C(28) phenyl carbon, in good agreement with the spectroscopic results. In this geometrical arrangement, one of the faces of the plane containing the metal atom and the chlorido and acetonitrile ligands becomes shielded by the phenyl rings of the phosphano fragment. This feature, similar to that found in the cation of compound **3** (see Figure 2), is relevant from the point of view of potential catalytic applications.

In order to elucidate the selective formation of compounds **7**-**10**, the structures and relative free energies of the cations **V**-**VIII** have been calculated (Figure 8). The acetonitrile solvato cations **VIIIa/b** −with the acetonitrile molecule *trans* to the aminic nitrogen atom− and their isomers **VIIa/b** −with the acetonitrile molecule *trans* to the

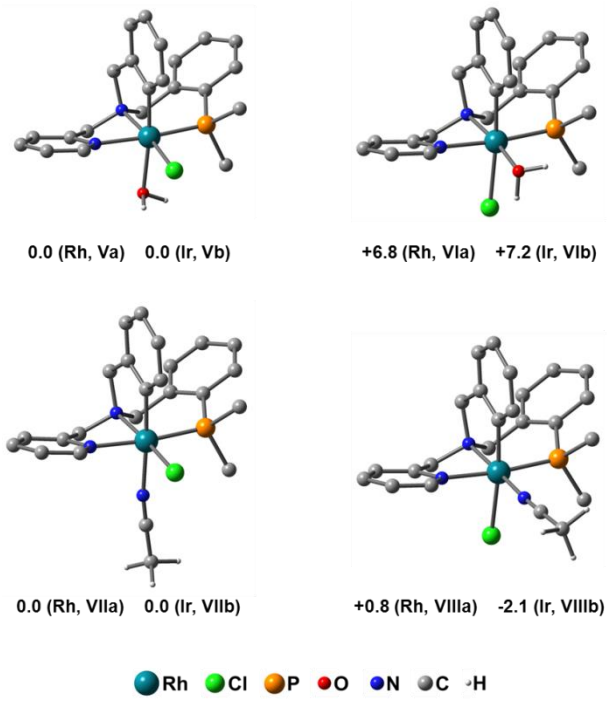

Figure 8. Structures and relative free energies (*G*, kcal·mol^{-1}, 298 K, CH_2Cl_2) of isomers **V**-**VIII** of [MCl(κ^4*C,N,N',P*-**L**)(Solv)]$^+$ (M = Rh, Ir; Solv = H_2O, MeCN). Only the structures with M = Rh are shown, those with M = Ir being similar. For clarity, most hydrogen atoms are omitted and only *ipso* carbons of the PPh_2 moiety are shown.

carbon atom– feature similar calculated stabilities. Thus, a kinetic control can be envisaged in the selective formation of **9** and **10**. In order to confirm this hypothesis, the relative stabilities of the putative 16-electron intermediates [MCl(κ^4*C,N,N',P*–**L**)]$^+$ (**IXa/b, Xa/b**) were calculated (Figure 9). The cations **IXa** and **Xa** (**IXb** and **Xb**) exhibit significantly different stabilities (ΔG > 15 kcal·mol^{-1}). In addition, a relaxed PES scan showed that the chlorido ligand abstraction from both **1** and **2** is a barrierless process leading to **IXa**/**b** or **Xa**/**b** (see SI). On this background, it can be reasonably argued that besides a higher *trans* influence (vide supra), the metalated carbon atom in **1** and **2** exerts a higher *trans* effect than the aminic nitrogen atom, thus preventing the observation and isolation of the cations **Xa/b** and allowing the isolation of only the isomers of **9** and **10** with the acetonitrile *trans* to the carbon atom.[20]

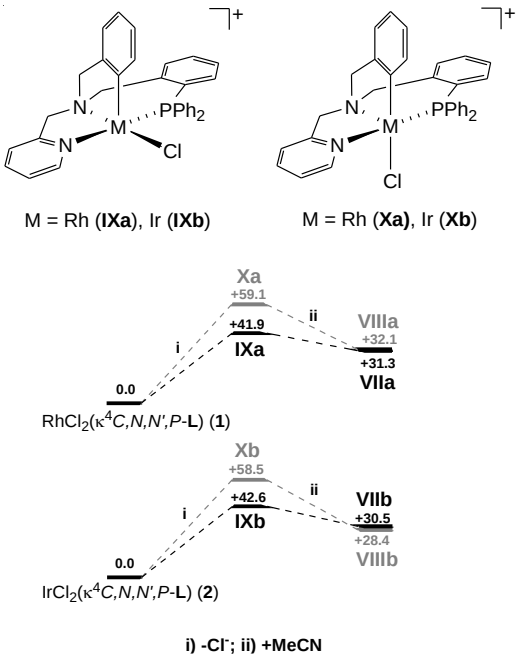

Figure 9. Cations [MCl(κ⁴*C,N,N',P*-**L**)]⁺ (**IXa/b**, **Xa/b**) and free energy profiles (*G*, kcal·mol⁻¹, 298 K, CH_2Cl_2) for the reaction [MCl_2(κ⁴*C,N,N',P*-**L**)] + MeCN → [MCl(κ⁴*C,N,N',P*-**L**)(NCMe)]⁺ + Cl^- (M = Rh, Ir).

Finally, when dealing with the formation of compounds **7** and **8**, the aquo complexes **VIa/b** (H_2O *trans* to nitrogen, Figure 8) were calculated to be less stable (+6.8, Rh; +7.2 kcal·mol⁻¹, Ir) than the corresponding isomers **Va/b** (H_2O *trans* to carbon). Thus, the clean formation of **7** and **8** should be the consequence of both the lower free energy of the putative intermediates **IXa/b** vs. **Xa/b** and the higher stability of **Va/b** vs. **VIa/b**.

Reaction of the dichlorido complexes 1 and 2 with $AgSbF_6$ in 2/3 molar ratio

At room temperature, acetonitrile suspensions of the complexes **1** and **2** reacted with $AgSbF_6$, in 2/3 molar ratio, affording the silver containing compounds [{M(κ⁴*C,N,N',P*–**L**)(NCMe)(*μ*-Cl)}$_2$Ag][SbF_6]$_3$ (M = Rh (**11**), Ir (**12**)) (Eq. 4a). These compounds were also isolated from dichloromethane/acetonitrile solutions of the acetonitrile complexes **9** and **10** containing $AgSbF_6$, in 2/1 molar ratio (Eq. 4b).

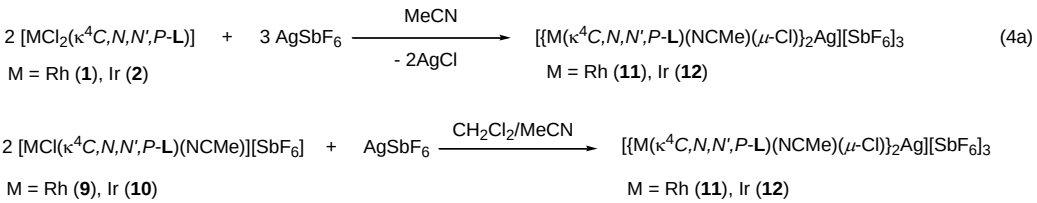

Crystals suitable for X-ray analysis were obtained from dichloromethane solutions of the complexes. As most of the features of the two crystals are similar, we will discuss here the molecular structure of the rhodium complex **11**. For details about the molecular structure of the iridium complex **12** see SI.

A view of the molecular structure of the cation of the complex is depicted in Figure 10 and relevant characteristics of the metal coordination spheres are summarized in Table 5. In the cation, two distorted-octahedral Rh(κ^4*C,N,N',P*–**L**)(NCMe)Cl fragments are bridged by a silver atom. The two halves of the cation are related by a 2-fold rotation axis passing through the silver atom. The complex crystallizes in the *C2/c* centrosymmetric space group and, therefore, pairs of enantiomeric cations **11**/**11'** are

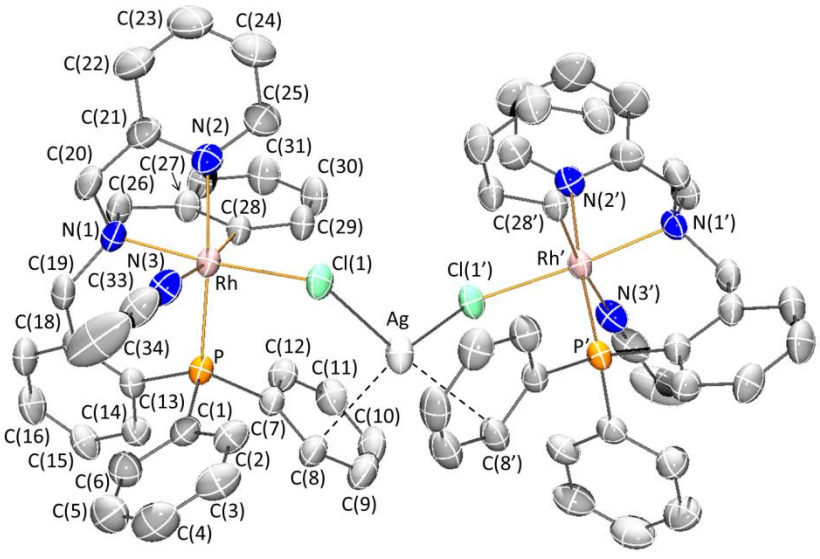

Figure 10. Molecular structure of the cation of complex **11** (thermal ellipsoids at a 30% probability level). Only the enantiomer with (*R*$_{Nam}$)-*OC*-6-54-*C* configuration in both rhodium fragments is shown. The configuration of the silver center is *Δ* (see text). For clarity hydrogen atoms have been omitted. Primed atoms are related to the unprimed one by the symmetry transformation 1−*x*, *y*, ½−*z*.

Table 5. Bond lengths (Å) and angles (°) for complex **11/11'.**

Rh-Cl(1)	2.3869(13)	P-Rh-N(1)	94.78(13)
Rh-P	2.2753(14)	P-Rh-N(2)	175.37(14)
Rh-N(1)	2.079(4)	P-Rh-N(3)	91.33(15)
Rh-N(2)	2.089(5)	P-Rh-C(28)	93.93(15)
Rh-N(3)	2.178(5)	N(1)-Rh-N(2)	80.65(18)
Rh-C(28)	2.007(5)	N(1)-Rh-N(3)	90.85(18)
Ag-Cl(1)	2.5360(15)	N(1)-Rh-C(28)	84.14(18)
Cl(1)-Rh-P	90.83(5)	N(2)-Rh-N(3)	89.5(2)
Cl(1)-Rh-N(1)	174.35(13)	N(2)-Rh-C(28)	84.9(2)
Cl(1)-Rh-N(2)	93.75(14)	N(3)-Rh-C(28)	173.02(19)
Cl(1)-Rh-N(3)	88.40(14)	Cl(1)-Ag-Cl(1')	120.19(8)
Cl(1)-Rh-C(28)	96.10(14)		

present in the unit cell. Only the cation of the unprimed isomer **11** is shown in Figure 10. Within each cation both rhodium moieties adopt the same absolute configuration i. e. both present (R_{Nam})-*OC*-6-54-*C* (**11**) or (S_{Nam})-*OC*-6-54-*A* (**11'**) configurations.

Notably, while the chlorido ligand *trans* to the phenyl carbon in the starting compound [$RhCl_2(\kappa^4$*C,N,N',P*–**L**)] (**1**) has been substituted by a MeCN molecule in complex **11**, the chlorido ligand *trans* to the aminic nitrogen remained coordinated to the rhodium atom, in spite of its interaction with a silver cation. The distance of 4.2552(6) Å between Rh and Ag excludes any significant intermetallic interaction.

The Ag−Cl bond length is 2.5360(15) Å and a Cl−Ag−Cl angle of 120.19(8)° was found. As far as we know, only four previous structures exhibit unsupported X_2Ag (X = halogen atom) bridges. Remarkably, in three of them, namely, $(NBu_4)_x[\{Pt(C_6Cl_5)_2(\mu\text{-}Cl)\}_2Ag]_x$,[21] $[\{PtCl(Me)(N,N\text{-chelate})(\mu\text{-}Cl)\}_2Ag]$,[22] and $[\{Ru_2(ap)_4(\mu\text{-}Cl)\}_2Ag]$,[23] linear Cl−Ag−Cl bridges are present, while the compound $[\{TpRe(N\text{-}p\text{-tol})\text{-}(Ph)(\mu\text{-}I)\}_2Ag]$ exhibits a smaller angle (124.3°).[24] In the latter, the silver atom additionally interacts with two carbon atoms of two aromatic rings, each one belonging to one of the two mononuclear subunits (Ag−C, 2.528(13) Å) completing a distorted-tetrahedral

environment for the silver. In a similar manner, in complex **11**, the silver atom lies at a relatively short distance of the aromatic C(8) and C(8') carbon atoms (2.711(6) Å).

The resulting stereochemistry on the silver center deserves some comments. Taking into account the two Ag···C attractive interactions, the silver cation presents a distorted-tetrahedral geometry. Furthermore, the two rhodium fragments Rh(κ^4*C,N,N',P*–**L**)(NCMe)Cl, each one acting as a "chelate ligand" through the Cl and one carbon atom, create a chiral environment around the silver atom. The relative spatial arrangement of these two chelates defines a *Δ* or *Λ* configuration for the silver center (Figure 11).[25] Taking into account that metallic fragments of R_N,C_{Rh} and S_N,A_{Rh} configuration are present in the solution, three pairs of enantiomeric diastereomers,

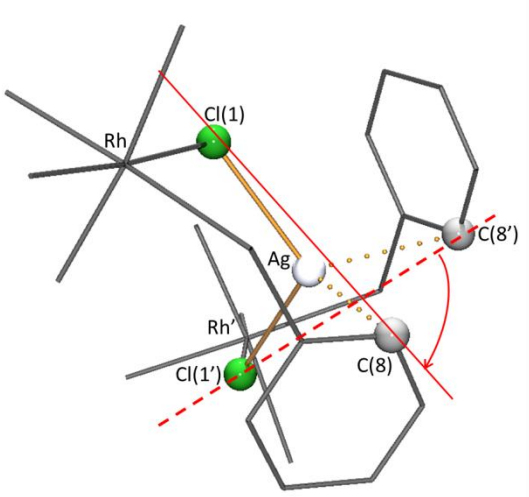

Figure 11. Assignment of the *Δ* configuration to the silver center in complex **11**.

namely, R_N,C_{Rh},*Δ*,$R_{N'}$,$C_{Rh'}$ / S_N,A_{Rh},*Λ*,$S_{N'}$,$A_{Rh'}$; R_N,C_{Rh},*Δ*,$S_{N'}$,$A_{Rh'}$ / S_N,A_{Rh},*Λ*,$R_{N'}$,$C_{Rh'}$ and S_N,A_{Rh},*Δ*,$S_{N'}$,$A_{Rh'}$ / R_N,C_{Rh},*Λ*,$R_{N'}$,$C_{Rh'}$ could form. Notably, only the pair of enantiomers R_N,C_{Rh},*Δ*,$R_{N'}$,$C_{Rh'}$ / S_N,A_{Rh},*Λ*,$S_{N'}$,$A_{Rh'}$ was isolated R-X polvo; Referencia en Footnote al espectro ^{31}P del sólido. Thus, the configuration at the silver center is predetermined,[5d,e] i. e., the silver atom only adopts a *Δ* configuration when joints R_N,C_{Rh} (**11**) moieties and a *Λ* configuration when is surrounded by two S_N,A_{Rh} (**11'**) fragments. The remaining

possible diastereomers were detected neither in solution (from 300 to 183 K) nor in the solid state.

The rhodium acetonitrile nitrogen bond length (Rh−N(3)) is 2.178(5) Å, comparable to that found in the bis-acetonitrile complex **3** (Rh−N(4) = 2.187(4) Å) for the acetonitrile *trans* to the sp^2 carbon atom. The bridging chlorido ligand is *trans* to an aminic nitrogen. Its Rh−Cl bond length, 2.3869(13) Å, is slightly longer than that found in [$RhCl_2$(κ^4*C,N,N',P*−**L**)], 2.3636(13) Å,[6] and in complex **5**, 2.36235(6) Å, for chlorido ligands also *trans* to aminic nitrogen atoms, but occupying terminal coordination positions.

The solid state structure of complexes **11** and **12** is not maintained in solution. ^{1}H, ^{13}C and ^{31}P{^{1}H} NMR spectra of their solutions in CD_2Cl_2 closely resemble those of the corresponding mononuclear cation in [MCl(κ^4*C,N,N',P*−**L**)(NCMe)][SbF_6] (M = Rh (**9**), Ir (**10**)). Hence, we propose that in solution the complexes dissociate according to the equilibrium depicted in Scheme 6. In fact, the hydrodynamic radii, evaluated by DOSY experiments, for dichloromethane solutions of the complexes **11** and **12** exhibit values of 5.11 (**11**) and 5.19 Å (**12**) and their diffusion coefficients are similar to that of the related mononuclear compounds **9** and **10** ($(D_t)_{9}/(D_t)_{11}$ and $(D_t)_{10}/(D_t)_{12}$ ratio, 1.06 and 1.02, respectively, see Table 3).

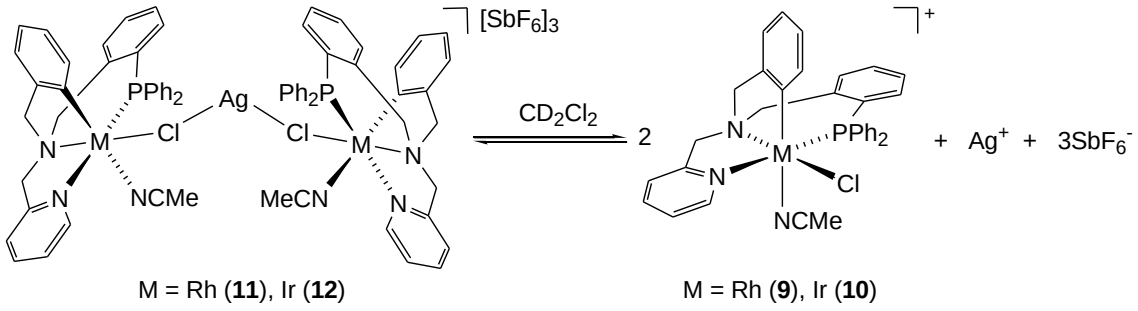

Scheme 6. Solution equilibrium for complexes **11** and **12**.

Finally, treatment of the complexes [{M(κ^4*C,N,N',P*–**L**)(NCMe)(*μ*-Cl)}$_2$Ag][SbF$_6$]$_3$ (M = Rh (**11**), Ir (**12**)) with equimolar amounts of AgSbF$_6$, at 80 ºC, in dichloromethane/acetonitrile, afforded the mononuclear acetonitrile complexes [M(κ^4*C,N,N',P*–**L**)(NCMe)$_2$][SbF$_6$]$_2$ (M = Rh (**3**), Ir (**4**)), according to NMR measurements (Eq. 5).

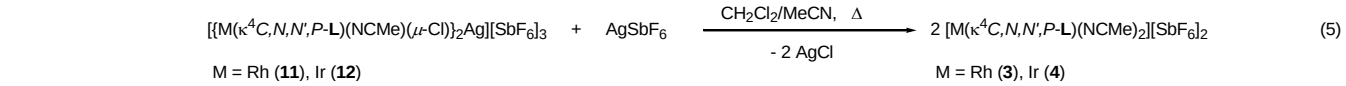

(5)

Regarding the stereochemical features of the new complexes **3**-**12**, it is interesting to note that all of them present only two distinct arrangements for the four ligating atoms in the M(κ^4*C,N,N',P*–**L**) entity. Each one corresponds to each one of the two isolated enantiomers of the compounds. Inversion of the chirality at the metal and at the aminic nitrogen atoms are two interconnect phenomena that take place concomitantly. For inverting the configuration at these centers, at least three M–**L** and/or N$_{am}$–C bonds have to be broken and, therefore, we speculate that this inversion must be a high energy-demanding process. Consequently, it may be envisaged that these metallic compounds are configurationally stable and, therefore, no changes on their configuration can be expected under the usual catalytic conditions.

DFT calculations on complexes 11 and 12

As mentioned above, the solid state structure of the cations [{M(κ^4*C,N,N',P*–**L**)(NCMe)(*μ*-Cl)}$_2$Ag]$^{3+}$ (M = Rh, Ir) reversibly breaks up upon dissolving and only one among three pairs of diasteroisomers is isolated namely, the pair *R*$_N$,*C*$_M$,*Δ*,*R*$_{N'}$,*C*$_{M'}$/*S*$_N$,*A*$_M$,*Λ*,*S*$_{N'}$,*A*$_{M'}$ (vide supra) R-X polvo. In order to gain insight into the selective formation of **11** and **12**, the structures of the three possible (pairs of)

diasteroisomers were elucidated by computational methods. The optimized structures of diasteroisomers **XI**-**XIII** and their relative energies are given in Figure 12.[26]

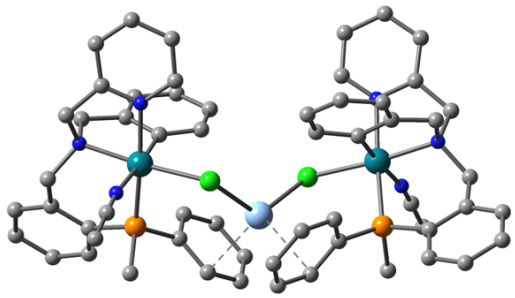

$R_N, C_M, \Delta, R_{N'}, C_{M'}$ **(XI)**
0.0 (Rh) 0.0 (Ir)

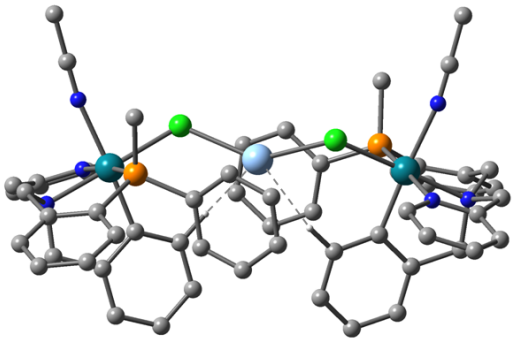

$R_N, C_M, \Lambda, R_{N'}, C_{M'}$ **(XII)**
+5.5 (Rh) +5.3 (Ir)

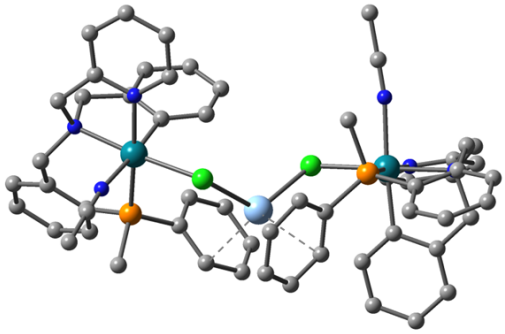

$R_N, C_M, \Delta, S_{N'}, A_{M'}$ **(XIII)**
+4.2 (Rh) +4.7 (Ir)

Figure 12. Structures and relative energies of isomers **XI**-**XIII** of [{M(κ^4*C,N,N',P*−**L**)(NCMe)(*μ*-Cl)}$_2$Ag]$^{3+}$ (M = Rh, Ir). For brevity only the structures with M = Rh are shown, those with M = Ir being similar. For clarity all hydrogen atoms are omitted and only the *ipso* carbon of the PPh moiety apart from silver is shown.

Interestingly, for **XI** and **XIII** the Cl−Ag−Cl moiety features a bent angle (126-127º) and similar Ag−Cl bond lengths (2.54-2.56 Å). In addition, short interatomic Ag···C distances have been observed between silver and one of the PPh group (2.66-2.72 Å), rendering a pseudo-tetrahedral coordination geometry around the metal. When dealing with **XII**, a different environment was observed for the silver. Indeed, a wider Cl−Ag−Cl angle (M = Rh, 144.3º; M = Ir, 138.6º) is observed along with slightly shorter Ag−Cl bond lengths (M = Rh, 2.49 Å; M = Ir, 2.51 Å). Further, the shortest Ag···C interatomic distances between the silver atom and the PPh_2 moiety are significantly longer (M = Rh, 3.15 Å; M = Ir, 3.09 Å) than those observed in **XI** and **XIII**. Additionally, short C-H···Ag interatomic distances (M = Rh, 2.49 Å; M = Ir, 2.43 Å) have been observed between the silver atom and both metalated phenyl rings. In spite of these structural differences, for the sake of comparison the *Λ*-configuration of the silver atom in **XII** has been assigned considering the closest PPh ring and the chlorido ligands.

The most stable enantiomer **XI** features the R_N,C_M configuration at both MCl(κ^4*C,N,N',P*−**L**)(NCMe) moieties and a *Δ* configuration of the silver atom, thus nicely fitting in with the solid state structure of the cation [{M(κ^4*C,N,N',P*−**L**)(NCMe)(*μ*-Cl)}$_2$Ag]$^{3+}$ in **11** and **12**. It is worth noting that, at variance with **5** and **6**, the most stable diasteroisomer **XI** does not present unique intramolecular interactions that can be considered responsible for its higher stability. Indeed, as mentioned before, besides the Ag−Cl bonds, the diasteroisomers feature Ag···C contacts (**XI**, **XIII**) and Ag···HC interactions (**XIII**), thus ruling out that the origin of the higher stability of **XI** vs. **XII** and **XIII** is the presence of the Ag···C interactions observed in the solid state and confirmed by DFT calculations. Alternatively, it can be argued that simply a better match-up among two (R_N,C_M)-MCl(κ^4*C,N,N',P*−**L**)(NCMe) fragments and a silver ion, rendering a *Δ*

environment for the latter, should be the basis of the higher stability of **XI** and, eventually, of the formation of the isolated isomers of the compounds **11** and **12**.

Conclusions

In summary, the abstraction of the two chlorido ligands in complexes **1** and **2** takes place in a sequential and selective manner. The chlorido *trans* to the carbon atom of the phenyl ring is removed preferentially to the one *trans* to the aminic nitrogen. While the former is replaced at room temperature, the abstraction of the latter requires harder conditions such as 80 ºC and the presence of donor solvents. This difference allows for the detection and characterization of the chlorido-bridged complexes **5** and **6**, the mononuclear mono-solvato compounds **7**-**10** and the silver containing trimetallic derivatives **11** and **12**. Notably, the formation of the intermediates **5**, **6** and **11**, **12** takes place with chiral self-recognition: only complexes containing monometallic fragments with the same absolute configuration have been detected. Moreover, the configuration of the chiral silver center present in complexes **11** and **12** is predetermined by the configuration of the involved rhodium or iridium fragments. DFT calculations support that π···π stacking interactions between the two pyridine rings in compounds **5** and **6**, also experimentally detected by NMR spectroscopy and X-ray crystallography, should be considered responsible for the molecular recognition observed in these compounds. However, a better match-up among two (R_N,C_M)−MCl(κ^4*C,N,N',P*−**L**)(NCMe) fragments and a silver cation, rendering a *Δ* environment for the latter (and, obviously, also among two (S_N,A_M)−MCl(κ^4*C,N,N',P*−**L**)(NCMe) fragments giving a *Λ* environment for the silver) should be responsible of the higher stability of the observed isomers and explain the preferential formation of the isolated isomers R-X polvo of complexes **11** and **12**.

On the other hand, no geometrical isomerization was observed over the whole process from the dichlorido **1**/**2** to the bis-solvato **3**/**4** complexes and the encountered stereochemistries hint that the absolute configuration is retained within monometallic fragments based on the M(κ^4*C,N,N',P*–**L**) unit. Consequently, with the tetracoordinate ligand **L** it would be possible to generate species with two *cis* substitutionally labile coordination positions but, in a rather paradoxical way, stereochemically stable. Hence, after optical resolution, these species would be excellent candidates for catalyst precursors in enantioselective catalysis. We are currently attempting the resolution of these complexes with the intention of applying them in asymmetric transformations.

Experimental Section

General

All preparations have been carried out under argon, unless otherwise stated. All solvents were treated in a PS-400-6 Innovative Technologies Solvent Purification System (SPS). Infrared spectra were recorded on Perkin-Elmer Spectrum-100 (ATR mode) FT-IR spectrometer. Carbon, hydrogen and nitrogen analyses were performed using a Perkin-Elmer 240 B microanalyzer. ^{1}H, ^{13}C and ^{31}P spectra were recorded on a Varian UNITY 300, a Bruker AV-300 (300.13 MHz), a Bruker AV-400 (400.16 MHz) or a Bruker AV-500 (500.13 MHz) spectrometers. Chemical shifts are expressed in ppm up field from $SiMe_4$ or 85% H_3PO_4 (^{31}P). *J* values are given in Hz. COSY, NOESY, HSQC, HMQC, and HMBC ^{1}H-X (X = ^{1}H, ^{13}C, ^{31}P) correlation spectra were obtained using standard procedures. DOSY experiments were carried out using the PFGSE (Pulsed-Field Gradient Spin-Echo) NMR Diffusion methods and analyzed with the software implemented by Bruker on a NMR AV500 spectrometer. Hydrodynamic radii (r_H) were calculated from the Stokes-Einstein equation: $r_H = kT/6\pi\eta D_t$, where T is the absolute temperature, *k* is the Boltzmann constant, η is the solvent viscosity and D_t is the translational self-diffusion coefficient. Mass spectra were obtained with a Micro Tof-Q Bruker Daltonics spectrometer.

Preparation and characterization of the complexes [M(κ⁴*C,N,N',P*–L)(NCMe)₂][SbF₆]₂ (M = Rh (3) Ir (4))

Compound **3**: To a solution of [$RhCl_2$(κ⁴*C,N,N',P*–**L**)] (400.0 mg, 0.620 mmol) in 20 mL of acetonitrile, 425.9 mg (1.240 mmol) of $AgSbF_6$ were added. The resulting suspension was placed under reflux 40 h and then was filtered to remove any insoluble material. The resulting clear yellow solution was evaporated to ca. 1 mL. Slow addition of Et_2O led to

the precipitation of a pale yellow solid that was filtered off, washed with Et_2O (2 × 3 mL) and vacuum-dried. Yield: 643.4 mg (92 %). Compound **4**: In a sealed tube, to a suspension of [$IrCl_2$(κ^4*C,N,N',P*–**L**)] (500.0 mg, 0.681 mmol) in 20 mL of acetonitrile, 467.6 mg (1.361 mmol) of $AgSbF_6$ were added. The resulting suspension was heated at 130 ºC for 4 days and then was filtered to remove any insoluble material. The resulting clear yellow solution was evaporated to ca. 1 mL. Slow addition of Et_2O led to the precipitation of a crystalline pale yellow solid that was filtered off, washed with Et_2O (2 × 3 mL) and vacuum-dried. Yield: 643.4 mg (79 %).

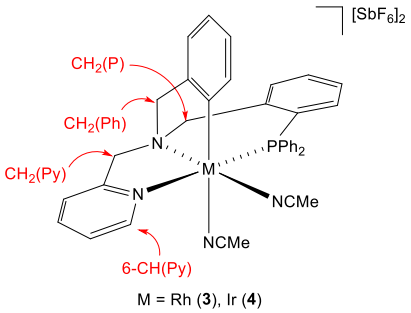

Compound **3**. Anal. calcd. $C_{36}H_{34}F_{12}N_4PRhSb_2 \cdot 2H_2O$: C, 37.70; H, 3.14; N, 4.89. Found: C, 37.30; H, 2.98; N, 4.82. IR (solid, cm^{-1}): ν(CN) 2310 (br), ν(SbF_6) 654 (s). HRMS (μ-TOF): $C_{36}H_{34}F_{12}N_4PRhSb_2$ $[M-SbF_6-MeCN]^+$: calc. 850.0248, found 850.0280. *^{1}H NMR (500.13 MHz, CD_2Cl_2, RT, ppm):* δ = 8.40 (brpt, *J* = 4.6 Hz, 1H, 6-CH(Py)), 7.99 (ptd, *J* = 7.8, 1.5 Hz, 1H, H(Ar)), 7.80 (ptpt, *J* = 7.8, 1.5 Hz, 1H, H(Ar)), 7.77-7.65 (m, 5H, H(Ar)), 7.61-7.49 (m, 3H, H(Ar)), 7.40 (m, 2H, H(Ar)), 7.31 (m, 2H, H(Ar)), 7.25 (ddd, *J* = 10.8, 7.8, 0.9 Hz, 1H, H(Ar)), 6.87 (m, 2H, H(Ar)), 6.78 (brpt, *J* = 9.4 Hz, 2H, H(Ar)), 6.54 (brdd, *J* = 7.1, 1.9 Hz, 1H, 6-CH(Ph)), 6.50 (brdd, *J* = 7.0, 2.3 Hz, 1H, H(Ar)), 5.15 (d, *J* = 15.9 Hz, 1H, *pro-S*-CH_2(Py)), 4.67 (d, *J* = 14.0 Hz, 1H, *pro-R*-CH_2(P)), 4.65 (d, *J* = 15.9 Hz, 1H, *pro-R*-CH_2(Py)), 4.54 (d, *J* = 17.4 Hz, 1H, *pro-R*-CH_2(Ph)), 4.44 (ddd, *J* = 14.0, 5.2, 1.8 Hz, 1H, *pro-S*-CH_2(P)), 3.90 (d, *J* = 17.4 Hz, 1H, *pro-S*-CH_2(Ph)), 2.64 (s, 3H, NCMe *cis* to C), and 1.98 (s, 3H, NCMe *trans* to C). *$^{13}C\{^1H\}$*

NMR (125.77 MHz, CD_2Cl_2, RT, ppm): δ = 156.12 (d, *J* = 2.0 Hz, 2-C(Py)), 149.80 (s, 6-CH(Py)), 147.06 (s, 2-C(Ph)), 146.79 (brdd, $J_{Rh\text{-}C}$ = 27.5 Hz, $J_{P\text{-}C}$ = 7.9 Hz, CRh), 141.45 (s, CH(Ar)), 139.83 (d, *J* = 16.7 Hz, 2-C(PhP)), 135.69 (d, *J* = 2.5 Hz, CH(Ar)), 135.19 (d, *J* = 9.6 Hz, CH(Ar)), 134.80 (d, *J* = 2.5 Hz, CH(Ar)), 134.50 (d, *J* = 9.3 Hz, 2C, CH(Ar)), 134.16 (d, *J* = 9.4 Hz, 2C, CH(Ar)), 133.99 (s, 6-CH(Ph)), 133.39 (d, *J* = 2.8 Hz, CH(Ar)), 133.06 (d, *J* = 2.8 Hz, CH(Ar)), 131.33 (d, *J* = 8.2 Hz, CH(Ar)), 130.24 (d, *J* = 10.7 Hz, 2C, CH(Ar)), 129.05 (d, *J* = 11.4 Hz, 2C, CH(Ar)), 128.80 (s, CH(Ar)), 127.18 (d, *J* = 3.5 Hz, CH(Ar)), 126.71 (d, $J_{Rh\text{-}C}$ = 5.9 Hz, N*C*Me *cis* to C), 125.98 (s, CH(Ar)), 125.85 (d, *J* = 50.4 Hz, C(Ar)), 124.29 (brs, N*C*Me *trans* to C), 124.18 (d, *J* = 2.4 Hz, CH(Ar)), 123.51 (d, *J* = 59.8 Hz, C(Ar)), 121.64 (d, *J* = 56.5 Hz, C(Ar)), 121.16 (s, CH(Ar)), 74.76 (s, CH_2(Py)), 67.75 (d, *J* = 8.2 Hz, CH_2(P)), 66.96 (s, CH_2(Ph)), 4.54 (s, NC*Me cis* to C), and 3.28 (brs, NC*Me trans* to C). *$^{31}P\{^1H\}$ NMR (202.46 MHz, CD_2Cl_2, RT, ppm):* δ = 28.75 (d, *J* = 116.3 Hz).

Compound **4**. Anal. calcd. $C_{36}H_{34}F_{12}IrN_4PSb_2 \cdot CH_2Cl_2$: C, 34.13; H, 2.78; N, 4.30. Found: C, 33.92; H, 2.66; N, 4.43. IR (solid, cm^{-1}): ν(CN) 2320 (br), ν(SbF_6) 653 (s). HRMS (μ-TOF): $C_{36}H_{34}F_{12}IrN_4PSb_2$ $[M-SbF_6-MeCN]^+$: calc. 940.0775, found 940.0817. *^1H NMR (500.13 MHz, CD_2Cl_2, RT, ppm):* δ = 8.45 (dddd, *J* = 5.7, 3.3, 1.4, 0.7 Hz, 1H, 6-CH(Py)), 8.01 (ptd, *J* = 7.8, 1.5 Hz, 1H, H(Ar)), 7.83-7.65 (m, 6H, H(Ar)), 7.58-7.47 (m, 3H, H(Ar)), 7.39-7.28 (m, 4H, H(Ar)), 7.20 (ddd, *J* = 11.2, 7.8, 1.2 Hz, 1H, H(Ar)), 6.85-6.72 (m, 4H, H(Ar)), 6.51 (brd, *J* = 7.3 Hz, 1H, H(Ar)), 6.45 (brd, *J* = 7.6 Hz, 1H, 6-CH(Ph)), 5.12 (d, *J* = 15.8 Hz, 1H, *pro-S*-CH_2(Py)), 4.97 (d, *J* = 15.6 Hz, 1H, *pro-R*-CH_2(Py)), 4.94 (d, *J* = 13.1 Hz, 1H, *pro-R*-CH_2(P)), 4.86 (dd, *J* = 13.8, 3.1 Hz, 1H, *pro-S*-CH_2(P)), 4.61 (d, *J* = 17.3 Hz, 1H, *pro-R*-CH_2(Ph)), 3.86 (d, *J* = 17.3 Hz, 1H, *pro-S*-CH_2(Ph)), 2.81 (d, *J* = 0.5 Hz, 3H, NCMe *cis* to C), and 2.07 (s, 3H, NCMe *trans* to C). *$^{13}C\{^1H\}$ NMR (125.77 MHz, CD_2Cl_2, RT, ppm):* δ = 156.95 (brs, 2-C(Py)), 149.29 (s, 6-CH(Py)), 148.53 (s, 2-

C(Ph)), 141.71 (s, CH(Ar)), 139.69 (d, *J* = 15.1 Hz, 2-C(PhP)), 135.28 (s, CH(Ar)), 135.24 (d, *J* = 7.8 Hz, CH(Ar)), 134.53 (s, CH(Ar)), 134.37 (d, *J* = 9.6 Hz, 2C, CH(Ar)), 133.85 (d, *J* = 9.3 Hz, 2C, CH(Ar)), 133.24 (s, 6-CH(Ph)), 133.19 (s, CH(Ar)), 132.86 (brs, CH(Ar)), 131.34 (d, *J* = 8.9 Hz, CH(Ar)), 130.18 (d, *J* = 10.7 Hz, 2C, CH(Ar)), 128.96 (d, *J* = 11.6 Hz, 2C, CH(Ar)), 127.61 (s, CH(Ar)), 127.39 (brs, CH(Ar)), 126.86 (brd, $J_{P\text{-}C}$ = 8.1 Hz, CIr), 125.63 (s, CH(Ar)), 125.06 (d, *J* = 58.7 Hz, C(Ar)), 124.15 (brs, CH(Ar)), 123.76 (s, N*C*Me *trans* to C), 123.02 (d, *J* = 66.2 Hz, C(Ar)), 121.47 (brs, N*C*Me *cis* to C), 121.35 (d, *J* = 62.7 Hz, C(Ar)), 120.18 (s, CH(Ar)), 76.64 (s, CH_2(Py)), 69.72 (s, CH_2(Ph)), 69.22 (d, *J* = 7.5 Hz, CH_2(P)), 4.57 (s, NC*Me cis* to C), and 3.54 (brs, NC*Me trans* to C). *$^{31}P\{^1H\}$ NMR (202.5 MHz, CD_2Cl_2, RT, ppm):* δ = –12.20 (s).

Preparation and characterization of the complexes [{MCl(κ^4*C,N,N',P*–L)}$_2$(*μ*-Cl)][SbF_6] (M = Rh (5), Ir (6))

At room temperature, to a solution of the corresponding complex [MCl_2(κ^4*C,N,N',P*–**L**)] (100.0 mg; 0.155 mmol (Rh), 0.136 mmol (Ir)) in 10 mL of CH_2Cl_2, 0.078 mmol (Rh) or 0.068 mmol (Ir) of $AgSbF_6$ were added. The resulting suspension was stirred for 2 h and then was filtered to remove the AgCl formed. Keeping at room temperature the filtrate, pale yellow crystals of the rhodium complex **5** were formed (yield: 72.4 mg, 63 %). Evaporating to dryness the filtrate, pure yellow samples of the iridium compound **6** were obtained (yield: 93.7 mg, 97 %).

Compound **5**. Anal. calcd. for $C_{64}H_{56}Cl_3F_6N_4P_2Rh_2Sb$: C, 51.56; H, 3.79; N, 3.76. Found: C, 51.34; H, 3.72; N, 3.32. IR (solid, cm^{-1}): ν(SbF_6) 651 (s). HRMS (μ-TOF): $C_{64}H_{56}Cl_3F_6N_4P_2Rh_2Sb$ $[M-SbF_6]^+$: calc. 1255.1126, found 1255.1124. *^1H NMR (500.13 MHz, CD_2Cl_2, RT, ppm):* δ = 7.92 (brs, 2H, 6-CH(Py)), 7.70-7.46 (m, 12H, H(Ar)), 7.35-

7.18 (m, 10H, H(Ar)), 6.74 (m, 6H, H(Ar)), 6.81 (d, *J* = 7.9 Hz, 2H, 6-CH(Ph)), 6.81 (br, 2H, H(Ar)), 6.61 (brs, 4H, H(Ar)), 6.55 (pt, *J* = 7.2 Hz, 2H, H(Ar)),

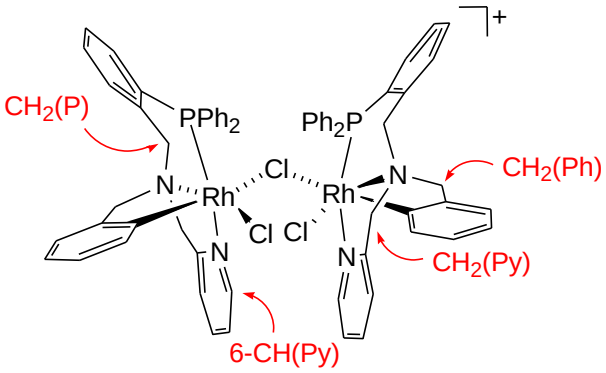

M = Rh (**5**), Ir (**6**)

6.38 (pt, *J* = 7.6, 1.5 Hz, 2H, H(Ar)), 6.30 (brd, *J* = 7.7 Hz, 2H, H(Ar)), 6.00 (brd, *J* = 13.9 Hz, 2H, CH_2(Py)), 4.79 (brd, *J* = 14.0 Hz, 2H, CH_2(P)), 4.37 (d, *J* = 17.1 Hz, 2H, CH_2(Ph)), 4.12 (brd, *J* = 14.5 Hz, 2H, CH_2(Py)), 43.79 (brd, *J* = 13.9 Hz, 2H, CH_2(P)), and 3.65 (d, *J* = 17.3 Hz, 2H, CH_2(Ph)). *$^{13}C\{^1H\}$ NMR (125.77 MHz, CD_2Cl_2, RT, ppm):* δ = 158.38 (d, *J* = 2.1 Hz, 2C, 2-C(Py)), 151.82 (br, 2C, CRh), 148.61 (s, 2C, 6-CH(Py)), 146.97 (s, 2C, 2-C(Ph)), 142.06 (d, *J* = 17.5 Hz, 2C, 2-C(PhP)), 138.37 (s, 2C, CH(Ar)), 137.06 (s, 2C, CH(Ar)), 135.32 (brs, 2C, 6-CH(Ph)), 135.04 (brd, *J* = 8.6 Hz, 4C, CH(Ar)), 134.24 (d, *J* = 8.8 Hz, 4C, CH(Ar)), 133.75 (d, *J* = 9.4 Hz, 2C, CH(Ar)), 133.11 (d, *J* = 2.2 Hz, 2C, CH(Ar)), 130.51 (d, *J* = 50.7 Hz, 2C, C(Ar)), 130.31 (brs, 4C, CH(Ar)), 129.65 (d, *J* = 6.8 Hz, 2C, CH(Ar)), 129.58 (brd, *J* = 59.1 Hz, 2C, C(Ar)), 128.54 (d, *J* = 10.4 Hz, 4C, CH(Ar)), 127.50 (d, *J* = 10.8 Hz, 4C, CH(Ar)), 127.33 (s, 2C, CH(Ar)), 125.44 (d, *J* = 48.7 Hz, 2C, C(Ar)), 124.99 (d, *J* = 3.8 Hz, 2C, CH(Ar)), 123.55 (s, 2C, CH(Ar)), 122.65 (d, *J* = 2.5 Hz, 2C, CH(Ar)), 119.73 (s, 2C, CH(Ar)), 75.21 (s, 2C, CH_2(Py)), and 68.58 (brs, 4C, CH_2(P), CH_2(Ph)). *$^{31}P\{^1H\}$ NMR (202.46 MHz, CD_2Cl_2, RT, ppm):* δ = 31.60 (d, *J* = 128.1 Hz, 2P).

Compound **6**. Anal. calcd. for $C_{64}H_{56}Cl_3F_6Ir_2N_4P_2Sb \cdot 1.5CH_2Cl_2$: C, 43.78; H, 3.31; N, 3.12. Found: C, 43.96; H, 3.30; N, 3.22. IR (solid, cm^{-1}): ν(SbF_6) 653 (s). HRMS (μ-TOF): $C_{64}H_{56}Cl_3F_6N_4P_2Ir_2Sb$ $[M-C_{32}H_{28}Cl_2F_6IrN_2PSb]^+$: calc. 699.1295, found 699.1288. *^{1}H NMR (500.13 MHz, CD_2Cl_2, RT, ppm):* δ = 7.97 (brpt, *J* = 3.8 Hz, 2H, 6-CH(Py)), 7.72 (ptd, *J* = 7.7, 1.5 Hz, 2H, H(Ar)), 7.63 (brpt, *J* = 7.5 Hz, 2H, H(Ar)), 7.58 (brd, *J* = 7.8 Hz, 2H, H(Ar)), 7.53-7.42 (m, 6H, H(Ar)), 7.36-7.29 (m, 6H, H(Ar)), 7.26 (brptd, *J* = 7.4, 1.8 Hz, 2H, H(Ar)), 7.20 (brpt, *J* = 7.4 Hz, 2H, H(Ar)), 6.94 (brptd, *J* = 8.2, 2.7 Hz, 4H, H(Ar)), 6.88 (brpt, *J* = 9.6 Hz, 2H, H(Ar)), 6.83 (brpt, *J* = 6.5 Hz, 2H, H(Ar)), 6.59 (m, 4H, H(Ar)), 6.57 (d, *J* = 7.9 Hz, 2H, 6-CH(Ph)), 6.50 (brptd, *J* = 7.4, 0.9 Hz, 2H, H(Ar)), 6.35-6.27 (m, 4H, H(Ar)), 5.87 (d, *J* = 14.7 Hz, 2H, CH_2(Py)), 4.87 (d, *J* = 13.8 Hz, 2H, CH_2(P)), 4.33 (d, *J* = 16.8 Hz, 2H, CH_2(Ph)), 4.30 (d, *J* = 14.7 Hz, 2H, CH_2(Py)), 4.11 (brd, *J* = 13.8 Hz, 2H, CH_2(P)), and 3.55 (d, *J* = 16.9 Hz, 2H, CH_2(Ph)). *^{13}C{^{1}H} NMR (125.77 MHz, CD_2Cl_2, RT, ppm):* δ = 159.32 (s, 2C, 2-C(Py)), 147.96 (s, 2C, 2-C(Ph)), 147.71 (s, 2C, 6-CH(Py)), 141.72 (d, *J* = 15.7 Hz, 2C, 2-C(PhP)), 138.50 (s, 2C, CH(Ar)), 136.58 (s, 2C, CH(Ar)), 135.01 (d, *J* = 8.5 Hz, 4C, CH(Ar)), 134.10 (d, *J* = 8.8 Hz, 4C, CH(Ar)), 133.68 (s, 2C, 6-CH(Ph)), 133.65 (d, *J* = 9.0 Hz, 2C, CH(Ar)), 132.92 (brs, 2C, CH(Ar)), 130.24 (brs, 4C, CH(Ar)), 130.03 (d, *J* = 59.2 Hz, 2C, C(Ar)), 129.95 (d, *J* = 7.4 Hz, 2C, CH(Ar)), 128.98 (d, *J* = 7.3 Hz, 2C, CIr), 128.90 (d, *J* = 64.2 Hz, 2C, C(Ar)), 128.51 (d, *J* = 10.4 Hz, 4C, CH(Ar)), 127.45 (d, *J* = 10.8Hz, 4C, CH(Ar)), 126.28 (s, 2C, CH(Ar)), 125.29 (d, *J* = 3.0 Hz, 2C, CH(Ar)), 125.27 (d, *J* = 56.4 Hz, 2C, C(Ar)), 123.39 (s, 2C, CH(Ar)), 122.64 (brs, 2C, CH(Ar)), 118.88 (s, 2C, CH(Ar)), 77.86 (s, 2C, CH_2(Py)), 69.55 (s, 2C, CH_2(Ph)), and 67.53 (d, *J* = 4.0 Hz, 2C, CH_2(P)). *^{31}P{^{1}H} NMR (202.46 MHz, CD_2Cl_2, RT, ppm):* δ = –12.47 (s, 2P).

Preparation and characterization of the complexes [MCl(κ^4*C,N,N',P*–L)(OH$_2$)][SbF$_6$] (M = Rh (7), Ir (8))

At room temperature, to a solution of the corresponding [MCl$_2$(κ^4*C,N,N',P*–**L**)] (150.0 mg; 0.232 mmol (Rh), 0.204 mmol (Ir)) in 10 mL of wet CH_2Cl_2, 0.232 mmol (Rh) or 0.204 mmol (Ir) of $AgSbF_6$ were added. The pale yellow suspension was stirred for 2 h and then was filtered to remove the AgCl formed. The light yellow filtrate was evaporated to dryness to afford the complexes [MCl(κ^4*C,N,N',P*–**L**)(OH$_2$)][SbF$_6$] (M = Rh (**7**), Ir (**8**)) as microcrystalline solids. Yield: 160.6 mg, 80 % (**7**); 188.7 mg, 97 % (**8**).

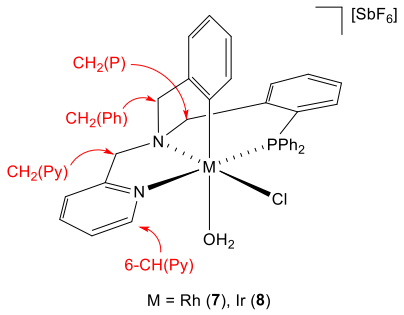

Compound **7**. Anal. calcd. for $C_{32}H_{30}ClF_6N_2OPRhSb$: C, 44.50; H, 3.50; N, 3.24. Found: C, 44.60; H, 3.69; N, 3.46. IR (solid, cm^{-1}): ν(SbF$_6$) 651 (s). HRMS (μ-TOF): $C_{32}H_{30}ClF_6N_2OPRhSb$ [M−SbF$_6$−H$_2$O]$^+$: calc. 609.0728, found 609.0711. *^{1}H NMR (500.13 MHz, CD$_2$Cl$_2$, RT, ppm):* δ = 8.94 (brpt, *J* = 4.3 Hz, 1H, 6-CH(Py)), 7.91 (ptd, *J* = 7.8, 1.5 Hz, 1H, H(Ar)), 7.80-7.35 (m, 11H, H(Ar)), 7.26 (ptd, *J* = 8.0, 3.0 Hz, 2H, H(Ar)), 7.20 (d, *J* = 8.0 Hz, 1H, 6-CH(Ph)), 7.13 (ddd, *J* = 10.0, 7.9, 0.7 Hz, 1H, H(Ar)), 6.85-6.65 (m, 4H, H(Ar)), 6.41 (brdd, *J* = 7.6, 1.5 Hz, 1H, H(Ar)), 5.03 (d, *J* = 15.4 Hz, 1H, *pro-S*-CH$_2$(Py)), 4.66 (d, *J* = 13.7 Hz, 1H, *pro-R*-CH$_2$(P)), 4.50 (d, *J* = 15.6 Hz, 1H, *pro-R*-CH$_2$(Py)), 4.47 (d, *J* = 17.4 Hz, 1H, *pro-R*-CH$_2$(Ph)), 4.36 (ddd, *J* = 13.7, 4.3, 1.6 Hz, 1H, *pro-S*-CH$_2$(P)), 3.82 (d, *J* = 17.3 Hz, 1H, *pro-S*-CH$_2$(Ph)), and 2.51 (s, 2H, OH$_2$ *trans* to C). *^{13}C{^{1}H} NMR (125.77 MHz, CD$_2$Cl$_2$, RT, ppm):* δ = 157.20 (brs, 2-C(Py)), 149.369 (s, 6-CH(Py)), 147.48 (brs, 2-C(Ph)), 145.14 (br, CRh), 140.59 (s, CH(Ar)),

140.20 (d, *J* = 16.8 Hz, 2-C(PhP)), 137.45 (s, 6-CH(Ph)), 135.89 (s, CH(Ar)), 134.97 (d, *J* = 9.5 Hz, 2C, CH(Ar)), 134.74 (d, *J* = 8.9 Hz, CH(Ar)), 134.24 (d, *J* = 8.5 Hz, 2C, CH(Ar)), 133.77 (s, CH(Ar)), 132.72 (s, CH(Ar)), 131.79 (s, CH(Ar)), 130.91 (d, *J* = 6.6 Hz, CH(Ar)), 130.45 (d, *J* = 10.2 Hz, 2C, CH(Ar)), 128.14 (d, *J* = 11.4 Hz, 2C, CH(Ar)), 127.43 (s, CH(Ar)), 126.43 (d, *J* = 46.6 Hz, C(Ar)), 125.99 (brs, CH(Ar)), 125.52 (d, *J* = 60.3 Hz, C(Ar)), 124.72 (d, *J* = 50.8 Hz, C(Ar)), 124.59 (s, CH(Ar)), 123.25 (s, CH(Ar)), 120.32 (s, CH(Ar)), 73.22 (s, CH_2(Py)), 67.51 (brd, *J* = 7.3 Hz, CH_2(P)), and 65.55 (s, CH_2(Ph)). *$^{31}P\{^1H\}$ NMR (202.46 MHz, CD_2Cl_2, RT, ppm):* δ = 31.75 (d, *J* = 128.9 Hz).

Compound **8**. Anal. calcd. for $C_{32}H_{30}ClF_6IrN_2OPSb \cdot H_2O$: C, 39.58; H, 3.32; N, 2.88. Found: C, 39.15; H, 3.31; N, 3.11. IR (solid, cm^{-1}): ν(SbF_6) 650 (s). HRMS (μ-TOF): $C_{32}H_{30}ClF_6IrN_2OPSb$ $[M-SbF_6-H_2O]^+$: calc. 699.1295, found 699.1304. *^1H NMR (500.13 MHz, CD_2Cl_2, RT, ppm):* δ = 9.00 (brpt, *J* = 4.0 Hz, 1H, 6-CH(Py)), 7.93 (ptd, *J* = 7.8, 1.5 Hz, 1H, H(Ar)), 7.74-7.36 (m, 11H, H(Ar)), 7.22 (ptd, *J* = 7.8, 2.7 Hz, 2H, H(Ar)), 7.02 (dd, *J* = 10.5, 8.1 Hz, 1H, H(Ar)), 6.99 (d, *J* = 7.9 Hz, 1H, 6-CH(Ph)), 6.80 (dd, *J* = 11.1, 8.3 Hz, 2H, H(Ar)), 6.67 (ptd, *J* = 7.3, 0.9 Hz, 1H, H(Ar)), 6.61 (brpt, *J* = 7.3 Hz, 1H, H(Ar)), 6.40 (brd, *J* = 7.4 Hz, 1H, H(Ar)), 5.01 (d, *J* = 15.4 Hz, 1H, *pro-S*-CH_2(Py)), 4.95 (d, *J* = 13.6 Hz, 1H, *pro-R*-CH_2(P)), 4.77 (dd, *J* = 13.6, 2.4 Hz, 1H, *pro-S*-CH_2(P)), 4.74 (d, *J* = 15.5 Hz, 1H, *pro-R*-CH_2(Py)), 4.48 (d, *J* = 17.0 Hz, 1H, *pro-R*-CH_2(Ph)), 3.74 (d, *J* = 17.0 Hz, 1H, *pro-S*-CH_2(Ph)), and 2.51 (br, 2H, OH_2 *trans* to C). *$^{13}C\{^1H\}$ NMR (125.7 MHz, CD_2Cl_2, RT, ppm):* δ = 158.26 (d, *J* = 1.7 Hz, 2-C(Py)), 148.79 (s, 2-C(Ph)), 148.61 (s, 6-CH(Py)), 140.71 (s, CH(Ar)), 140.10 (d, *J* = 15.2 Hz, 2-C(PhP)), 136.50 (s, 6-CH(Ph)), 135.40 (d, *J* = 2.8 Hz, CH(Ar)), 134.89 (d, *J* = 9.3 Hz, 2C, CH(Ar)), 134.71 (d, *J* = 9.5 Hz, CH(Ar)), 133.93 (d, *J* = 9.1 Hz, 2C, CH(Ar)), 133.43 (brd, *J* = 1.5 Hz, CH(Ar)), 132.44 (brs, CH(Ar)), 131.58 (brs, CH(Ar)), 131.01 (d, *J* = 7.7

Hz, CH(Ar)), 130.41 (d, *J* = 10.5 Hz, 2C, CH(Ar)), 128.14 (d, *J* = 11.4 Hz, 2C, CH(Ar)), 126.23 (d, *J* = 53.7 Hz, C(Ar)), 126.13 (s, 2C, CH(Ar)), 125.39 (d, *J* = 66.9 Hz, C(Ar)), 124.80 (d, *J* = 59.0 Hz, C(Ar)), 124.21 (s, CH(Ar)), 123.19 (s, CH(Ar)), 119.89 (brs, CIr), 119.06 (s, CH(Ar)), 75.57 (s, CH_2(Py)), 69.43 (d, *J* = 5.8 Hz, CH_2(P)), and 68.57 (s, CH_2(Ph)). *$^{31}P\{^1H\}$ NMR (202.46 MHz, CD_2Cl_2, RT, ppm): δ* = −10.07 (s).

Preparation and characterization of the complexes [MCl(κ^4*C,N,N',P*–L)(NCMe)][SbF_6] (M = Rh (9), Ir (10))

At room temperature, to a solution of the corresponding [MCl_2(κ^4*C,N,N',P*–**L**)] (100.0 mg; 0.155 mmol (Rh), 0.136 mmol (Ir)) in 10 mL of MeCN, 0.155 mmol (Rh) or 0.136 mmol (Ir) of $AgSbF_6$ were added. The pale yellow suspension was stirred for 2 h and then was filtered to remove the AgCl formed. The light yellow filtrate was evaporated to dryness to afford the complexes [MCl(κ^4*C,N,N',P*–**L**)(NCMe)][SbF_6] (M = Rh (**9**), Ir (**10**)) as microcrystalline solids. Yield: 106.9 mg, 78 % (**9**); 99.6 mg, 75 % (**10**).

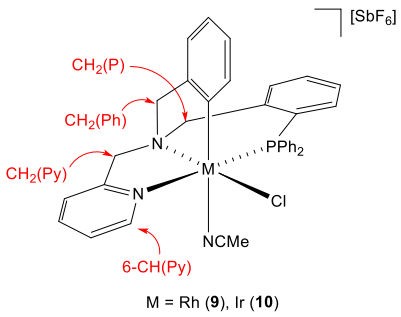

Compound **9**. Anal. calcd. $C_{34}H_{31}ClF_6N_3PRhSb$: C, 46.06; H, 3.52; N, 4.74. Found: C, 45.74; H, 3.55; N, 4.59. IR (solid, cm^{-1}): ν(SbF_6) 652 (s). HRMS (μ-TOF): $C_{34}H_{31}ClF_6N_3PRhSb$ $[M–SbF_6–MeCN]^+$: calc. 609.0728, found 609.0713. *^1H NMR (500.13 MHz, CD_2Cl_2, RT, ppm): δ* = 8.92 (brs, 1H, 6-CH(Py)), 7.90-7.78 (m, 3H, H(Ar)), 7.73-7.44 (m, 7H, H(Ar)), 7.42 (pt, *J* = 7.3 Hz, 2H, H(Ar)), 7.37 (pt, *J* = 6.4 Hz, 1H,

H(Ar)), 7.20 (d, *J* = 7.8 Hz, 1H, 6-CH(Ph)), 7.15 (brs, 2H, H(Ar)), 7.11 (pt, *J* = 8.9 Hz, 1H, H(Ar)), 6.77-6.65 (m, 3H, H(Ar)), 6.41 (d, *J* = 7.2 Hz, 1H, H(Ar)), 5.13 (d, *J* = 15.5 Hz, 1H, *pro*-*S*-CH_2(Py)), 4.82 (d, *J* = 13.9 Hz, 1H, *pro*-*R*-CH_2(P)), 4.56 (d, *J* = 15.5 Hz, 1H, *pro*-*R*-CH_2(Py)), 4.50 (d, *J* = 17.3 Hz, 1H, *pro*-*R*-CH_2(Ph)), 4.43 (brd, *J* = 13.9 Hz, 1H, *pro*-*S*-CH_2(P)), 3.81 (d, *J* = 17.3 Hz, 1H, *pro*-*S*-CH_2(Ph)), and 1.78 (s, 3H, NCMe *trans* to C). *$^{13}C\{^1H\}$ NMR (125.77 MHz, CD_2Cl_2, RT, ppm):* δ = 157.02 (s, 2-C(Py)), 149.35 (s, 6-CH(Py)), 149.28 (brdd, $J_{Rh\text{-}C}$ = 28.1 Hz, $J_{P\text{-}C}$ = 10.8 Hz, CRh), 148.46 (s, 2-C(Ph)), 140.60 (d, *J* = 16.5 Hz, 2-C(PhP)), 140.04 (s, CH(Ar)), 136.42 (s, 6-CH(Ph)), 136.82 (brs, CH(Ar)), 135.02 (d, *J* = 9.1 Hz, 2C, CH(Ar)), 134.77 (d, *J* = 9.3 Hz, 2C, CH(Ar)), 134.67 (d, *J* = 10.1 Hz, CH(Ar)), 133.61 (s, CH(Ar)), 131.93 (brs, CH(Ar)), 131.37 (brs, CH(Ar)), 130.57 (d, *J* = 7.2 Hz, CH(Ar)), 129.17 (d, *J* = 10.3 Hz, 2C, CH(Ar)), 128.92 (d, *J* = 50.2 Hz, C(Ar)), 127.79 (d, *J* = 11.2 Hz, 2C, CH(Ar)), 127.46 (s, CH(Ar)), 126.42 (d, *J* = 61.5 Hz, C(Ar)), 125.69 (d, *J* = 2.9 Hz, CH(Ar)), 124.86 (d, *J* = 51.0 Hz, C(Ar)), 124.32 (s, CH(Ar)), 123.15 (s, CH(Ar)), 121.50 (brs, N*C*Me *trans* to C), 119.71 (s, CH(Ar)), 74.31 (s, CH_2(Py)), 67.89 (brd, *J* = 6.3 Hz, CH_2(P)), 66.10 (s, CH_2(Ph)), and 32.99 (brs, NC*Me trans* to C). *$^{31}P\{^1H\}$ NMR (202.46 MHz, CD_2Cl_2, RT, ppm):* δ = 31.58 (d, *J* = 125.7 Hz).

Compound **10**. Anal. calcd. $C_{34}H_{31}ClF_6IrN_3PSb\cdot CH_2Cl_2$: C, 39.62; H, 3.13; N, 3.96. Found: C, 39.47; H, 3.23; N, 4.05. IR (solid, cm^{-1}): ν(CN) 2069 (br), ν(SbF_6) 652 (s). HRMS (μ-TOF): $C_{34}H_{31}ClF_6IrN_3PSb$ $[M–SbF_6–MeCN]^+$: calc. 699.1295, found 699.1305. To enhance the solubility, two drops of MeCN were added to the NMR tubes. *^1H NMR (400.16 MHz, CD_2Cl_2, RT, ppm):* δ = 8.97 (dddd, *J* = 5.7, 2.4, 1.6, 0.8 Hz, 1H, 6-CH(Py)), 7.90 (ptd, *J* = 7.8, 1.6 Hz, 1H, H(Ar)), 7.75-7.58 (m, 5H, H(Ar)), 7.58-7.48 (m, 3H, H(Ar)), 7.46-7.34 (m, 3H, H(Ar)), 7.15 (m, 2H, H(Ar)), 7.04 (d, *J* = 6.7 Hz, 1H, 6-CH(Ph)), 7.02 (m, 1H, H(Ar)), 6.79-6.59 (m, 4H, H(Ar)), 6.42 (brdd, *J* = 7.3, 1.4 Hz,

1H, H(Ar)), 5.07 (d, *J* = 13.3 Hz, 1H, *pro-R*-CH_2(P)), 5.06 (d, *J* = 15.9 Hz, 1H, *pro-S*-CH_2(Py)), 4.88 (dd, *J* = 13.7, 2.4 Hz, 1H, *pro-S*-CH_2(P)), 4.84 (d, *J* = 15.5 Hz, 1H, *pro-R*-CH_2(Py)), 4.50 (d, *J* = 17.1 Hz, 1H, *pro-R*-CH_2(Ph)), 3.72 (d, *J* = 17.1 Hz, 1H, *pro-S*-CH_2(Ph)), and 1.87 (brs, 3H, NCMe *trans* to C). *$^{13}C\{^1H\}$ NMR (100.62 MHz, CD_2Cl_2, RT, ppm):* δ = 158.01 (d, *J* = 1.8 Hz, 2-C(Py)), 150.00 (s, C(*i*-Ph)), 148.21 (s, 6-CH(Py)), 140.49 (d, *J* = 15.1 Hz, 2-C(PhP)), 140.17 (s, CH(Ar)), 135.68 (d, *J* = 3.3 Hz, CH(Ar)), 135.06 (s, 6-CH(Ph)), 134.87 (d, *J* = 9.1 Hz, 2C, CH(Ar)), 134.65 (d, *J* = 9.4 Hz, CH(Ar)), 134.40 (d, *J* = 9.1 Hz, 2C, CH(Ar)), 133.31 (d, *J* = 2.4 Hz, CH(Ar)), 131.68 (d, *J* = 2.6 Hz, CH(Ar)), 131.24 (d, *J* = 2.7 Hz, CH(Ar)), 130.69 (d, *J* = 7.9 Hz, CH(Ar)), 129.82 (d, *J* = 8.0 Hz, CIr), 129.10 (d, *J* = 10.4 Hz, 2C, CH(Ar)), 128.16 (d, *J* = 56.3 Hz, C(Ar)), 127.77 (d, *J* = 11.3 Hz, 2C, CH(Ar)), 126.25 (s, CH(Ar)), 125.97 (d, *J* = 66.4 Hz, C(Ar)), 125.82 (d, *J* = 3.3 Hz, CH(Ar)), 124.65 (d, *J* = 58.4 Hz, C(Ar)), 123.99 (s, CH(Ar)), 123.12 (d, *J* = 2.3 Hz, CH(Ar)), 120.74 (brs, N*C*Me *trans* to C), 118.80 (s, CH(Ar)), 76.79 (s, CH_2(Py)), 69.59 (d, *J* = 5.6 Hz, CH_2(P)), 69.17 (s, CH_2(Ph)), and 3.28 (s, NC*Me trans* to C). *$^{31}P\{^1H\}$ NMR (161.98 MHz, CD_2Cl_2, RT, ppm):* δ = −12.51 (s).

Preparation and characterization of the complexes [{M(κ^4*C,N,N',P*–L)(NCMe)(μ-Cl)}$_2$Ag][SbF$_6$]$_3$ (M = Rh (11), Ir (12))

At room temperature, to a solution of the corresponding [MCl_2(κ^4*C,N,N',P*–**L**)] (100.0 mg; 0.155 mmol (Rh), 0.136 mmol (Ir)) in 10 mL of MeCN, 0.232 mmol (Rh) and 0.204 mmol (Ir) of $AgSbF_6$ were added. The pale yellow suspension was stirred for 2 h and then was filtered to remove the AgCl formed. The light yellow filtrate was evaporated to dryness to afford the complexes [{M(κ^4*C,N,N',P*–**L**)(NCMe)(μ-Cl)}$_2$Ag][SbF_6]$_3$ (M = Rh (**11**), Ir (**12**)) as microcrystalline solids. Yield: 139.4 mg, 85 % (**11**); 148.3 mg, 95 % (**12**).

Crystal Structure Determination of Complexes 3, 5, 10, 11 and 12

X-ray diffraction data were collected with graphite-monochromated Mo Kα radiation (λ = 0.71073 Å) using narrow ω rotations (0.3º) at room temperature on a Bruker DUO diffractometer (complexes **3** and **11**), and at 100(2) K on a Bruker Smart APEX (complexes **5**, **10** and **12**). Data reduction was performed with APEX 2 package, intensities were integrated with SAINT+,[27] and corrected for absorption effects with SADABS[28] and TWINABS (compound **10**)[29] programs. The structures were solved by direct methods with SHEXLS-2013,[30] and refined by full-matrix least-squares refinement on F^2 with SHELXL-2014[31] included in WINGX package.[32] Hydrogen atoms have been included in the models in calculated positions and refined with a riding model to decrease the number of refined parameters. Particular details concerning the presence of solvent or disorder are listed below.

*Crystal data for complex **3***: $C_{36}H_{34}F_{12}N_4PRhSb_2 \cdot 2(H_2O)$; M = 1164.08; colourless prism, 0.090 × 0.144 × 0.155 mm^3; monoclinic, *C2/c*; a = 35.3605(16) Å, b = 10.1795(5) Å, c = 24.3560(11) Å, β = 96.1780(10)°; Z = 8; V = 8716.1(7) $Å^3$; D_c = 1.774 g/cm^3; μ = 1.729 mm^{-1}; min. and max. absorption correction factors 0.702 and 0.847; $2\theta_{max}$ = 58.048°; 47077 collected reflections, 11261 unique reflections; R_{int} = 0.0259; number of data/restraint/parameters 11261/0/506; final GoF 1.050; R_1 = 0.0541 [8202 reflections, $I > 2\sigma(I)$]; *wR2* = 0.1776 all data; largest difference peak 1.122 e·$Å^{-3}$. Fluorine atoms of SbF_6 and oxygen atoms of water have been found to be disordered. Two sets of positions have been defined with complementary occupancy factors (0.58/0.42(1); 0.55/0.45(1) and 0.52/0.48(2), respectively) and isotropically refined.

*Crystal data for complex **5***: $C_{64}H_{56}Cl_3F_6N_4P_2Rh_2Sb \cdot 4(CH_2Cl_2)$; M = 1830.69; yellow prism, 0.100 × 0.150 × 0.175 mm^3; monoclinic, $P2_1/n$; a = 13.0023(6) Å, b = 20.1071(9)

Å, c = 26.7211(12) Å, β = 90.9350(10)°; Z = 4; V = 6985.0(5) Å^3; D_c = 1.741 g/cm^3; μ = 1.379 mm^{-1}; min. and max. absorption correction factors 0.773 and 0.865; $2\theta_{max}$ = 57.666°; 99324 collected reflections, 17124 unique reflections; R_{int} = 0.0391; number of data/restraint/parameters 17124/1/856; final GoF 1.070; R_1 = 0.0309 [14541 reflections, $I > 2\ \sigma(I)$]; *wR2* = 0.0701 all data; largest difference peak 0.727 e·Å^{-3}. Chlorine atoms of a dichloromethane molecule have been included in three sets of positions and isotropically refined, as they have been found to be disordered.

Crystal data for complex ***10****:* $2(C_{34}H_{31}ClF_6N_3PIrSb)\cdot C_2H_3N$; M = 1993.03; colourless prism, 0.090 × 0.090 × 0.180 mm^3; monoclinic, $P2_1/n$; a = 14.9694(15) Å, b = 17.1360(17) Å, c = 27.399(3) Å, β = 91.3330(10)°; Z = 4; V = 7026.5(12) Å^3; D_c = 1.884 g/cm^3; μ = 4.7337 mm^{-1}; min. and max. absorption correction factors 0.592 and 0.746; $2\theta_{max}$ = 56.76°; 58942 collected reflections, 14613 unique reflections; R_{int} = 0.0659; number of data/restraint/parameters 14613/12/877; final GoF 1.006; R_1 = 0.0565 [9835 reflections, $I > 2\ \sigma(I)$]; *wR2* = 0.1034 all data; largest difference peak 1.625 e·Å^{-3}. Reflection data of complex **10** reveals the existence of two domains in the twinned crystal. Data for both domains have been integrated. The structural model has been refined with reflection data of domain 1.

Crystal data for complex ***11***: $C_{68}H_{62}AgCl_2F_{18}N_6P_2Rh_2Sb_3\cdot 2(CH_2Cl_2)$; M = 2286.86; yellow prism, 0.112 × 0.120 × 0.225 mm^3; monoclinic, $C2/c$; a = 19.1983(8) Å, b = 28.4389(12) Å, c = 16.5795(9) Å, β = 113.1180(10)°; Z = 4; V = 8325.2(7) Å^3; D_c = 1.825 g/cm^3; μ = 1.892 mm^{-1}; min. and max. absorption correction factors 0.721 and 0.809; $2\theta_{max}$ = 56.542°; 60624 collected reflections, 10239 unique reflections; R_{int} = 0.0366; number of data/restraint/parameters 10239/2/481; final GoF 1.034; R_1 = 0.0557 [7093 reflections, $I > 2\ \sigma(I)$]; *wR2* = 0.1809 all data; largest difference peak 1.283 e·Å^{-3}. The counterion and the solvent molecules were found to be disordered. Fluorine atoms of both

SbF_6 of the asymmetric unit were included in the model in two sets of positions with complementary occupancy factors (0.543/0.457(9) and 0.59/0.41(2), respectively) and isotropically refined. Similar strategy was used in the refinement of the carbon atom and one chlorine of CH_2Cl_2 with 0.52/0.48(2) occupancy factors. Geometrical restraints concerning C-Cl bond lengths were defined for the minority part.

Crystal data for complex ***12***: $C_{68}H_{62}AgCl_2F_{18}Ir_2N_6P_2Sb_3 \cdot 2(CH_2Cl_2)$; M = 2465.44; yellow prism, 0.086 × 0.102 × 0.194 mm^3; monoclinic, *C2/c*; a = 18.7285(9) Å, b = 28.6160(13) Å, c = 16.1348(13) Å, β = 112.4620(4)°; Z = 4; V = 7991.2(8) $Å^3$; D_c = 2.049 g/cm^3; μ = 4.885 mm^{-1}; min. and max. absorption correction factors 0.471 and 0.637; $2\theta_{max}$ = 55.754°; 51330 collected reflections, 9433 unique reflections; R_{int} = 0.0383; number of data/restraint/parameters 9433/1/498; final GoF 0.885; R_1 = 0.0291 [8106 reflections, $I > 2\sigma(I)$]; *wR2* = 0.0824 all data; largest difference peak 1.752 $e \cdot Å^{-3}$. Dichloromethane has been found to be disordered. A chlorine and the carbon atom have been included in the model in three sets of positions with 0.44/0.29/0.27(1) occupancy factors and isotropically refined.

CCDC 1538233-1538237 contain the supplementary crystallographic data for this paper. These data can be obtained free of charge from The Cambridge Crystallographic Data Centre.

DFT calculations. Molecular structure optimizations, relaxed PSE calculations and frequencies calculations were carried out with the Gaussian09 program (revision D.01)[33] using the method B3PW91,[34] including the D3 dispersion correction scheme by Grimme with Becke Johnson damping[35] The def2-SVP[36] basis and pseudo potential were used for all atoms and the "ultrafine" grid was employed in all calculations. Stationary points were characterized by vibrational analysis. All the structures were optimized in CH_2Cl_2

(298 K) using the PCM method,[37] except **XI**-**XIV** which were optimized in gas phase (298 K, 1 atm). Atomic coordinates of calculated structures and the energies of the relaxed PSE scan calculations are given in the SI.

Acknowledgments

We thank the Ministerio de Economía y Competitividad of Spain (CTQ2015-66079-P) and Gobierno de Aragón (Grupo Consolidado E-63: Catalizadores Organometálicos Enantioselectivos) for financial support. M. C. acknowledges Diputación General de Aragón, CSIC and European Social Fund for a grant. R. R. acknowledges the Ministerio de Economía y Competitividad of Spain for a Ramón y Cajal (RYC-2013-13800) grant. P. G.-O. acknowledges CSIC, European Social Fund and Ministerio de Economía y Competitividad of Spain for a PTA contract. V. P. thanks the resources of the supercomputer "Memento" and the technical expertise and assistance provided by the Institute for Biocomputation and Physics of Complex Systems (BIFI), Universidad de Zaragoza. We acknowledge Universidad de Zaragoza-Centro Universitario de la Defensa for financial support (UZCUD 20/6-CIE-05).

Keywords: chiral self-recognition · iridium · rhodium · stererochemistry · tetradentate ligands · *trans* influence

References and Notes

[1] a) *Comprehensive Asymmetric Catalysis*, Vol 1-3 (Eds.: E. N. Jacobsen, A. Pfaltz, H. Yamamoto), Springer, New York, **1999**; Suppl. 1 and 2, Springer, New York, **2004**; b) *Catalytic Asymmetric Synthesis* (Ed.: I. Ojima), VCH, Wiley-Weinheim, Germany, **2000**; c) R. Noyori in *Asymmetric Catalysis in Organic Synthesis*, John Wiley and Sons, New York, **1994**; d) P. J. Walsh, M. C. Kozlowski in

Fundamentals of Asymmetric Catalysis, University Science Books, Sausalito, **2009**; e) *Lewis Acids in Organic Synthesis*, (Ed.: H. Yamamoto) Wiley-VCH: Weinheim, **2000**; (f) *Transition Metals for Organic Synthesis: Building Blocks and Fine Chemicals*, 2nd Edition, (Eds.: M. Beller, C. Bolm), Wiley-VCH, **2008**.

[2] M. Fontecave, O. Hamelin, S. Ménage, *Top. Organomet. Chem*. **2005**, *15*, 271-288.

[3] See for example: a) T. Oguma, T. Katsuki, in *Transition Metal Catalysis in Aerobic Alcohol Oxidation*, Ch. 9: *Asymmetric Oxidation of Alcohols and Phenol Derivatives with Air as Oxidant*. From series: RSC Green Chemistry, **2015**, pp. 231-255; b) K. Matsumoto, B. Saito, T. Katsuki, *Chem. Commun*. **2007**, 3619-3627; c) J. F. Larrow, E. N. Jacobsen, *Top. Organomet. Chem*. **2004**, *6*, 123-152; d) T. Katsuki, *Synlett* **2003**, 281-297; e) T. Katsuki, *Adv. Synth. Catal.* **2002**, *344*, 131-147. f) E. N. Jacobsen, *Acc. Chem. Res.* **2000**, *33*, 421-431; g) L. Canali, D. C. Sherrington, *Chem. Soc. Rev*. **1999**, *28*, 85-93; h) T. Katsuki, *Coord. Chem. Rev.* **1995**, *140*, 189-214.

[4] See for example: a) Y.-Y. Li, S.-L. Yu, W.-Y. Shen, J.-X. Gao, *Acc. Chem. Res*. **2015**, *48*, 2587-2598; b) R. H. Morris, *Acc. Chem. Res*. **2015**, *48*, 1494-1502; c) A. Mezzetti, *Dalton Trans*. **2010**, *39*, 7851-7869; d) C. Bonaccorsi, A. Mezzetti, *Curr. Org. Chem*. **2006**, *10*, 225-240.

[5] See for example: a) O. Cussó, X. Ribas, M. Costas, *Chem. Commun*. **2015**, *51*, 14285-14298; b) W. A. Chomitz, J. Arnold, *Chem. Eur. J*. **2009**, *15*, 2020-2030; c) M. Hechavarría Fonseca, B. König, *Adv. Synth. Catal*. **2003**, *345*, 1173-1185; d) P. D. Knight, P. Scott, *Coord. Chem. Rev*. **2003**, *242*, 125-143; e) U. Knof, A. von Zelewsky, *Angew. Chem. Int. Ed*. **1999**, *38*, 302-322; *Angew. Chem*. **1999**, *111*,

312-333; f) J. R. Aldrich-Wright, R. S. Vagg, P. A. Williams, *Coord. Chem. Rev*. **1997**, *166*, 361-389.

[6] M. Carmona, R. Rodríguez, I. Méndez, V. Passarelli, F. J. Lahoz, P. García-Orduña, D. Carmona, *Dalton Trans*. **2017**, *46*, 7332-7350.

[7] a) R. S. Cahn, C. Ingold, V. Prelog, *Angew. Chem., Int. Ed. Engl*. **1966**, *5*, 385-415; *Angew. Chem*. **1966**, *5*, 413-447; b) V. Prelog, G. Helmchen, *Angew. Chem., Int. Ed. Engl*. **1982**, *21*, 567-583; *Angew. Chem.* **1982**, *94*, 614-631; c) C. Lecomte, Y. Dusausoy, J. Protas, J. Tirouflet, A. Dormond, *J. Organomet. Chem*. **1974**, *73*, 67-76. For the *C*/*A* convention for octahedral centers see: d) N. G. Connelly, T. Damhus, R. H. Hartshorn, A. T. Hutton, In *Nomenclature of Inorganic Chemistry*; IUPAC Recommendations **2005**, RSC Publishing, Cambridge, UK. Chapter IR-9.3.4.8, p. 189.

[8] To simplify the notation of the stereochemical descriptors, we will label these diastereomers as R_N,C_M and S_N,A_M. *R* and *S* refers to the configuration at the aminic nitrogen and *C* and *A* to the clockwise or anticlockwise arrangement of the donor atoms at the equatorial plane of the octahedral molecule.

[9] L. Zhang, E. Meggers, *Acc. Chem. Res*. **2017**, *50*, 320-330.

[10] a) D. Carmona, F. Viguri, F. J. Lahoz, L. A. Oro, *Inorg. Chem*. **2002**, *41*, 2385-2388; b) G. Sipos, P. Gao, D. Foster, B. W. Skelton, A. N. Sobolev, R. Dorta, *Organometallics*, **2017**, *36*, 801-817.

[11] Isomer **3**. Puckering parameters for a) metallacycle Rh-N(1)-C(20)-C(21)-N(2): q = 0.436(5) Å, Φ = 42.7(6)°, $E_2/^3T_2$ conformation; b) metallacycle Rh-N(1)-C(26)-C(27)-C(28): q = 0.032(5) Å, Φ = −86(7)°, $^4T_3$ conformation; c) metallacycle Rh-

P-C(13)-C(18)-C(19)-N(1): q = 0.653(4) Å, φ = −94.2(3)°, θ = 74.4(3)°, $^{5}S_{6}/^{2}T_{6}$ conformation.

[12] a) D. Cremer, J. A. Pople, *J. Am. Chem. Soc*. **1975**, *97*, 1354-1358; b) C. Giacovazzo, H. L. Monaco, G. Artioli, D. Viterbo, G. Ferraris, G. Gilli, C. M. Zanotti, in *Fundamentals of Crystallography*, 2nd ed.; Oxford University Press; Oxford, U. K., **2002**.

[13] a) C. R. Groom, I. J. Bruno, M. P. Lightfoot, S. C. Ward, *Acta Cryst.* **2016**, *B72*, 171-179; b) J. S. Merola, T. Le Husebo, H. E. Selnau, *Inorg. Chim. Acta* **2012**, *390*, 33-36.

[14] D. Cuervo, J. Díez, M. P. Gamasa, J. Gimeno, *Organometallics* **2005**, *24*, 2224-2232.

[15] F. Acha, M. A. Garralda, R. Hernández, L. Ibarlucea, E. Pinilla, M. R. Torres, M. Zarandona, *Eur. J. Inorg. Chem.* **2006**, 3893-3900.

[16] P. Paredes, J. Díez, M. P. Gamasa, J. Gimeno, *J. Organomet. Chem.* **2008**, *693*, 3681-3687.

[17] C. Janiak, *J. Chem. Soc., Dalton Trans*. **2000**, 3885-3896.

[18] a) P. S. Pregosin, P. G. A. Kumar, I. Fernández, *Chem. Rev*. **2005**, *105*, 2977-2998; b) A. Macchioni, G. Ciancaleoni, C. Zuccaccia, D. Zuccaccia, *Chem. Soc. Rev*. **2008**, *37*, 479-489.

[19] At 223 K, the ^{1}H and $^{31}P\{^{1}H\}$ NMR spectra of complex **5**, in wet CD_2Cl_2, show three broad small proton signals in the 8.7-9.2 ppm range assigned to 6-CH(Py) protons and three broad phosphorus signals in the 24-36 ppm region. The total relative abundance of these signals was less than 2 %. No better resolution was

achieved by further lowering the temperature until 183 K. We tentatively propose that these minor compounds are mixtures of isomers of the dinuclear species of formulae $[(\kappa^4 C,N,N',P–\mathbf{L})RhCl(\mu\text{-}Cl)(H_2O)Rh(\kappa^4 C,N,N',P–\mathbf{L})]^{2+}$ and/or $[(\kappa^4 C,N,N',P–\mathbf{L})Rh(\mu\text{-}Cl)_2Rh(\kappa^4 C,N,N',P–\mathbf{L})]^{2+}$ arising from the dissociation of the water molecule of the aquo-complex **7** and subsequent coupling of the resulting unsaturated fragments. The low abundance and poor resolution of these species preclude a more accurate structural characterization.

[20] Noteworthy, the isomerization **VIIa/b ⇆ VIIIa/b** via the dissociative sequence **VIIa/b ⇆** *SPY*-5-43-$[M(\kappa^4 C,N,N',P–\mathbf{L})(NCMe)]^{2+} + Cl^- \leftrightarrows$ *SPY*-5-53-$[M(\kappa^4 C,N,N',P–\mathbf{L})(NCMe)]^{2+} + Cl^-$ **⇆ VIIIa/b** should be ruled out. Indeed the *SPY*-5-53 and *SPY*-5-43 putative intermediates $[M(\kappa^4 C,N,N',P–\mathbf{L})(NCMe)]^{2+}$ (M = Rh, Ir) were calculated to be at $G > +50$ kcal·mol^{-1} (298 K, CH_2Cl_2) with respect **VIIa/b** thus definitively ruling out that pathway.

[21] R. Usón, J. Forniés, M. Tomás, J. M. Casas, F. A. Cotton, L. R. Falvello, *Inorg. Chem.* **1986**, *25*, 4519-4525.

[22] V. G. Albano, M. D. Serio, M. Monari, I. Orabona, A. Panunzi, F. Ruffo, *Inorg. Chem*. **2002**, *41*, 2672-2677.

[23] A. R. Corcos, J. F. Berry, *Dalton Trans*. **2016**, *45*, 2386-2389.

[24] W. S. McNeil, D. D DuMez, Y. Matano, S. Lovell, J. M. Mayer, *Organometallics* **1999**, *18*, 3715-3727.

[25] A. von Zelewsky in *Stereochemistry of Coordination Compounds*, John Wiley and Sons, Chichester, **1996**.

[26] The diasteroisomers **XI-XIII** contain two non-equivalent PPh groups for each PPh_2 moiety. Consequently, given the configurations of silver and of the MCl(κ^4*C,N,N',P*–**L**) moieties, different isomers exist depending on which PPh interacts with silver. The diasteroisomers shown in Figure 12 are the most stable, the others featuring energies >10.2 kcal·mol^{-1} with respect to **XI**.

[27] SAINT+, *version 6.01: Area-Detector Integration Software*, Bruker AXS, Madison, WI, **2001**.

[28] a) R. H. Blessing, *Acta Crystallogr*. **1995**, *A51*, 33-3; b) SADABS, *Area Detector Absorption Correction Program*, Bruker AXS, Madison, WI, **1996**.

[29] G. M. Sheldrick, **2012**. *TWINABS.* University of Göttingen, Germany.

[30] a) G. M. Sheldrick, *Acta Crystallogr.* **1990**, *A46*, 467-473; b) G. M. Sheldrick, *Acta Crystallogr.* **2008**, *A64*, 112-122.

[31] G. M. Sheldrick, *Acta Crystallogr.* **2015**, *C71*, 3-8.

[32] L. J. Farrugia, *Acta Crystallogr*. **2012**, *45*, 849-854.

[33] Gaussian 09, Revision D.01, M. J. Frisch, G. W. Trucks, H. B. Schlegel, G. E. Scuseria, M. A. Robb, J. R. Cheeseman, G. Scalmani, V. Barone, B. Mennucci, G. A. Petersson, H. Nakatsuji, M. Caricato, X. Li, H. P. Hratchian, A. F. Izmaylov, J. Bloino, G. Zheng, J. L. Sonnenberg, M. Hada, M. Ehara, K. Toyota, R. Fukuda, J. Hasegawa, M. Ishida, T. Nakajima, Y. Honda, O. Kitao, H. Nakai, T. Vreven, J. A. Montgomery, Jr. , J. E. Peralta, F. Ogliaro, M. Bearpark, J. J. Heyd, E. Brothers, K. N. Kudin, V. N. Staroverov, R. Kobayashi, J. Normand, K. Raghavachari, A. Rendell, J. C. Burant, S. S. Iyengar, J. Tomasi, M. Cossi, N. Rega, J. M. Millam, M. Klene, J. E. Knox, J. B. Cross, V. Bakken, C. Adamo, J. Jaramillo, R. Gomperts,

R. E. Stratmann, O. Yazyev, A. J. Austin, R. Cammi, C. Pomelli, J. W. Ochterski, R. L. Martin, K. Morokuma, V. G. Zakrzewski, G. A. Voth, P. Salvador, J. J. Dannenberg, S. Dapprich, A. D. Daniels, C. Farkas, J. B. Foresman, J. V. Ortiz, J. Cioslowski, D. J. Fox, Gaussian, Inc., Wallingford CT, 2009.

[34] J. P. Perdew, in *Electronic Structure of Solids '91*, Ed. P. Ziesche and H. Eschrig, Akademie Verlag, Berlin, 1991.

[35] S. Grimme, S. Ehrlich, L. Goerigk, *J. Comp. Chem*. **2011**, *32*, 1456-1465.

[36] F. Weigend, R. Ahlrichs, *Phys. Chem. Chem. Phys*. **2005**, *7*, 3297-3305.

[37] J. Tomasi, B. Mennucci, R. Cammi, *Chem. Rev*. **2005**, *105*, 2999-3093.

Entry for the Table of Contents

Let's go step by step The chlorido ligands in complexes $[MCl_2(\kappa^4 C,N,N',P–\mathbf{L})]$ (M = Rh, Ir) are sequentially removed to give bis-solvato complexes of formula $[M(\kappa^4 C,N,N',P–\mathbf{L})(NCMe)_2]^{2+}$. Involved mono, di and trimetallic intermediates are isolated and characterized. The formation of these intermediates takes place with chiral self-recognition R-X polvo. The stereochemistry determined for the new species is compatible with the retention of the configuration of the metallic fragments throughout the whole process.

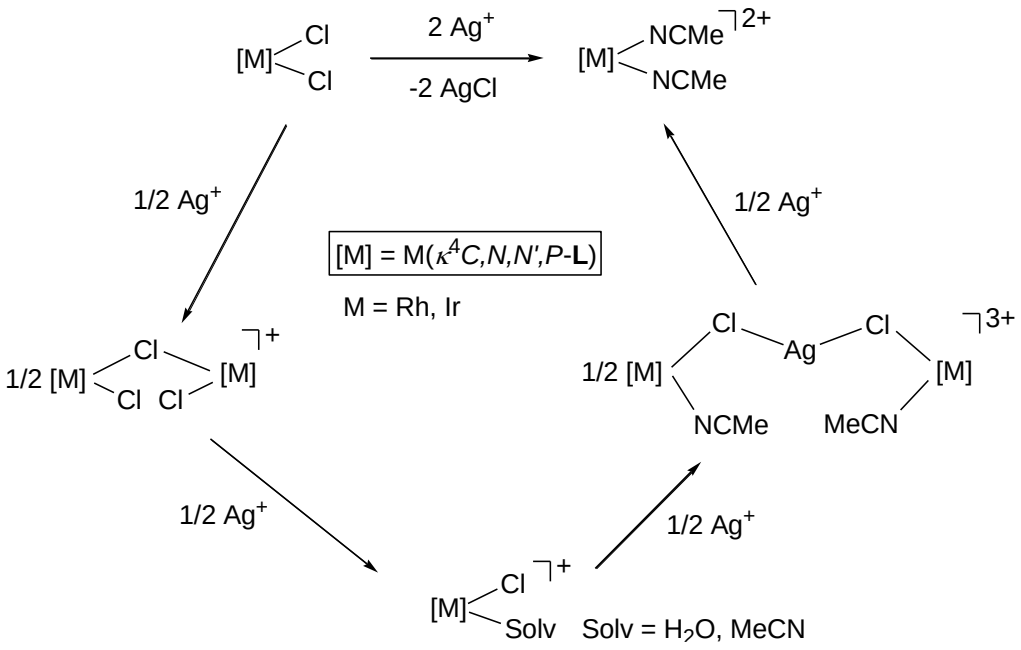

María Carmona,[a] Leyre Tejedor,[a] Ricardo Rodríguez,*[a] Vincenzo Passarelli,*[a,b] Fernando J. Lahoz,[a] Pilar García-Orduña[a] and Daniel Carmona*[a]

The Stepwise Reaction of Rhodium and Iridium Complexes of formula $[MCl_2(\kappa^4 C,N,N',P–\mathbf{L})]$ with Silver Cations: A Case of *trans*-Influence and Chiral Self-Recognition